GOETHE UNIVERSITÄT FRANKFURT AM MAIN

Low-energy limit of the $O(4)$ quark-meson model

Jürgen Eser, Florian Divotgey, Mario Mitter, and Dirk H. Rischke

Theory Center Seminar

JLab | September 26, 2018

Studienstiftung des deutschen Volkes

HGS-HIRe for FAIR
Helmholtz Graduate School for Hadron and Ion Research

Motivation: QCD at low energies

Chiral symmetry

Linear realization

Linear sigma model (LSM)
Extended LSM (eLSM)
Quark-meson model

Nonlinear realization

Chiral perturbation theory (ChPT)

Integration

Tree level
and
functional renormalization group (FRG)

Low-energy limit
same as for QCD?

Chiral perturbation theory (ChPT)

- Systematic analysis of **hadronic n-point functions** of QCD
  [Gasser, Leutwyler '84,'85; Leutwyler '94; etc.]
- Pion interactions dominate the low-energy regime
- **Chiral expansion:** Most general chiral-invariant Lagrangian with terms coupled by the low-energy couplings of QCD,

$$\begin{aligned}\mathcal{L}_{\mathrm{ChPT}} = & \frac{1}{2}\left(\partial_\mu \vec{\pi}\right)^2 - \frac{1}{2} m_\pi^2 \vec{\pi}^{\,2} + C_{1,\mathrm{ChPT}}\left(\vec{\pi}^{\,2}\right)^2 + C_{2,\mathrm{ChPT}}\left(\vec{\pi}\cdot\partial_\mu\vec{\pi}\right)^2 \\ & + C_{3,\mathrm{ChPT}}\left(\partial_\mu\vec{\pi}\right)^2\left(\partial_\nu\vec{\pi}\right)^2 + C_{4,\mathrm{ChPT}}\left(\partial_\mu\vec{\pi}\cdot\partial_\nu\vec{\pi}\right)^2 \\ & + \mathcal{O}\left(\pi^6, \partial^6\right)\end{aligned}$$

Extended linear sigma model (eLSM)

- Linear realization of chiral symmetry ("chiral partners")
- Applications at nonzero temperature and chemical potential
- Contains all $J^P = 0^\pm, 1^\pm$ mesons up to 2 GeV in mass
- **Representations** of $U(N_f)_r \times U(N_f)_l$:

$$\Phi \sim \bar{q}_r q_l \to U_l \, \Phi \, U_r^\dagger ,$$
$$R_\mu \sim \bar{q}_r \gamma_\mu q_r \to U_r R_\mu \, U_r^\dagger ,$$
$$L_\mu \sim \bar{q}_l \gamma_\mu q_l \to U_l L_\mu \, U_l^\dagger$$

- Vector and axial-vector mesons:

$$V_\mu = \frac{1}{2} \left(L_\mu + R_\mu \right) , \qquad A_\mu = \frac{1}{2} \left(L_\mu - R_\mu \right)$$

- **Disclaimer:** No attempt to compete with ChPT

eLSM Lagrangian

$$
\begin{aligned}
\mathcal{L}_{\mathrm{eLSM}} = \mathrm{tr}\left[\left(D^{\mu}\Phi\right)^{\dagger} D_{\mu}\Phi\right] - m_0^2\,\mathrm{tr}\left(\Phi^{\dagger}\Phi\right) \\
-\lambda_1\left[\mathrm{tr}\left(\Phi^{\dagger}\Phi\right)\right]^2 - \lambda_2\,\mathrm{tr}\left[\left(\Phi^{\dagger}\Phi\right)^2\right] \\
-\frac{1}{4}\,\mathrm{tr}\left(L_{\mu\nu}^2 + R_{\mu\nu}^2\right) + \mathrm{tr}\left[\left(\frac{m_1^2}{2} + \Delta\right)\left(L_{\mu}^2 + R_{\mu}^2\right)\right] \\
+\mathrm{tr}\left[H\left(\Phi + \Phi^{\dagger}\right)\right] - c_A\left(\det\,\Phi + \det\,\Phi^{\dagger}\right) \\
+i\frac{g_2}{2}\left(\mathrm{tr}\left\{L^{\mu\nu}\left[L_{\mu}, L_{\nu}\right]\right\} + \mathrm{tr}\left\{R^{\mu\nu}\left[R_{\mu}, R_{\nu}\right]\right\}\right) \\
+\frac{h_1}{2}\,\mathrm{tr}\left(\Phi^{\dagger}\Phi\right)\mathrm{tr}\left(L_{\mu}^2 + R_{\mu}^2\right) + h_2\,\mathrm{tr}\left(\left|L_{\mu}\Phi\right|^2 + \left|\Phi R_{\mu}\right|^2\right) \\
+2h_3\,\mathrm{tr}\left(\Phi R^{\mu}\Phi^{\dagger}L_{\mu}\right) + g_3\left[\mathrm{tr}\left(L^{\mu}L^{\nu}L_{\mu}L_{\nu}\right) + \mathrm{tr}\left(R^{\mu}R^{\nu}R_{\mu}R_{\nu}\right)\right] \\
+g_4\left[\mathrm{tr}\left(L^{\mu}L_{\mu}L^{\nu}L_{\nu}\right) + \mathrm{tr}\left(R^{\mu}R_{\mu}R^{\nu}R_{\nu}\right)\right] + g_5\,\mathrm{tr}\left(L^{\mu}L_{\mu}\right)\mathrm{tr}\left(R^{\nu}R_{\nu}\right) \\
+g_6\left[\mathrm{tr}\left(L^{\mu}L_{\mu}\right)\mathrm{tr}\left(L^{\nu}L_{\nu}\right) + \mathrm{tr}\left(R^{\mu}R_{\mu}\right)\mathrm{tr}\left(R^{\nu}R_{\nu}\right)\right],
\end{aligned}
$$

$$
D_{\mu}\Phi = \partial_{\mu}\Phi - ig_1\left(L_{\mu}\Phi - \Phi R_{\mu}\right), \qquad L_{\mu\nu} = \partial_{\mu}L_{\nu} - \partial_{\nu}L_{\mu}
$$

eLSM publications

- Introduction of the eLSM
  [Parganlija, Giacosa, Rischke '10;
  Parganlija, Kovacs, Wolf, Giacosa, Rischke '13]
- Chiral partner of the nucleon
  [Gallas, Giacosa, Rischke '10; Lakaschus, Mauldin, Giacosa, Rischke '18]
- Incorporating scalar glueball
  [Janowski, Giacosa, Rischke '14; Giacosa, Sammet, Janowski '17]
- Baryon multiplets
  [Olbrich, Zetenyi, Giacosa, Rischke '16,'18]
- Nonzero-temperature study within the FRG
  [JE, Grahl, Rischke '15]

$O(4)$ quark-meson model

- Two-flavor model, $N_f = 2$
- Specific limit of the eLSM
- **Euclidean** action:

$$S = \int_x \left\{ \frac{1}{2} \left(\partial_\mu \sigma \right) \partial_\mu \sigma + \frac{1}{2} \left(\partial_\mu \vec{\pi} \right) \cdot \partial_\mu \vec{\pi} + U(\rho) - h_{\mathrm{ESB}} \sigma \right.$$
$$\left. + \bar{\psi} \left(\gamma_\mu \partial_\mu + y \Phi_5 \right) \psi \right\},$$
$$\Phi_5 = \sigma t_0 + i \gamma_5 \vec{\pi} \cdot \vec{t},$$
$$\rho = \sigma^2 + \vec{\pi}^2$$

- **Explicit** and **spontaneous** symmetry breaking implemented,

$$h_{\mathrm{ESB}} \neq 0, \qquad \sigma \to \phi + \sigma$$

Integration at tree level

Low-energy limit of the eLSM

- Integrate out all fields, except pions,
  cf. [Divotgey, Kovacs, Giacosa, Rischke '18]

- Low-energy limit of the eLSM at **tree level**:

$$\mathcal{L}_{\mathrm{eLSM}} = \frac{1}{2}\left(\partial_\mu \vec{\pi}\right)^2 - \frac{1}{2} m_\pi^2 \vec{\pi}^{\,2} + C_{1,\mathrm{eLSM}} \left(\vec{\pi}^{\,2}\right)^2 + C_{2,\mathrm{eLSM}} \left(\vec{\pi} \cdot \partial_\mu \vec{\pi}\right)^2 + C_{3,\mathrm{eLSM}} \left(\partial_\mu \vec{\pi}\right)^2 \left(\partial_\nu \vec{\pi}\right)^2 + C_{4,\mathrm{eLSM}} \left(\partial_\mu \vec{\pi} \cdot \partial_\nu \vec{\pi}\right)^2 + \mathcal{O}\left(\pi^6, \partial^6\right)$$

- Match coefficients to ChPT,

$$\mathcal{L}_{\mathrm{ChPT}} = \frac{1}{2}\left(\partial_\mu \vec{\pi}\right)^2 - \frac{1}{2} m_\pi^2 \vec{\pi}^{\,2} + C_{1,\mathrm{ChPT}} \left(\vec{\pi}^{\,2}\right)^2 + C_{2,\mathrm{ChPT}} \left(\vec{\pi} \cdot \partial_\mu \vec{\pi}\right)^2 + C_{3,\mathrm{ChPT}} \left(\partial_\mu \vec{\pi}\right)^2 \left(\partial_\nu \vec{\pi}\right)^2 + C_{4,\mathrm{ChPT}} \left(\partial_\mu \vec{\pi} \cdot \partial_\nu \vec{\pi}\right)^2 + \mathcal{O}\left(\pi^6, \partial^6\right)$$

Tree-level low-energy couplings

Table 1: Comparison of the low-energy couplings at tree level, cf. [Bijnens, Ecker '14; Divotgey, Kovacs, Giacosa, Rischke '18].

Coupling	**ChPT**	**eLSM**
C_1	-0.28 ± 1.9	-0.268 ± 0.021
$C_2 \times 10^5$ MeV^2	5.882 ± 0.013	5.399 ± 0.081
$C_3 \times 10^{11}$ MeV^4	-5.61 ± 0.89	$-9.302 \pm 0.591 + \text{corr.}^{\text{a}}$
$C_4 \times 10^{11}$ MeV^4	2.51 ± 0.41	$9.448 \pm 0.589 + \text{corr.}^{\text{a}}$

[a] further corrections from undetermined model parameters

- **ChPT:** $C_1 = -M^2/(8f_\pi^2)$, $C_2 = 1/(2f_\pi^2)$, $C_3 = l_1/f_\pi^4$, $C_4 = l_2/f_\pi^4$
- **eLSM:** functions of model parameters m_0^2, λ_1, λ_2, h_1, h_2, h_3, g_1, ...

Open questions

- Tree-level calculation sufficient?
  Resonance saturation in low-energy constants,
  cf. [Ecker, Gasser, Pich, de Rafael '89]
- How do these values change if we include **loop corrections**?
- Can we produce similar values within the **FRG formalism**?
- **First step:** Exploratory study of higher-derivative couplings within the FRG formalism,
  cf. [JE, Divotgey, Mitter, Rischke, PRD 98 (2018) no.1, 014024]
- Following analysis restricted to the **$O(4)$ quark-meson model** as specific limit of the eLSM

Integration within the FRG

Functional renormalization group (FRG)

- Implementation of the **Wilsonian RG** idea
- Renormalization scale(k)-dependent **effective action** Γ_k
- FRG flow equation: [Wetterich '93]

$$\partial_k \Gamma_k = \frac{1}{2}\,\mathrm{tr}\left[\partial_k R_k \left(\Gamma_k^{(2)} + R_k\right)^{-1}\right] = \frac{1}{2}$$

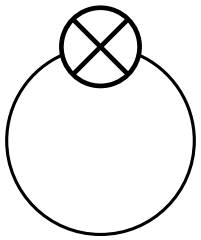

- Regulator function R_k provides correct integration limits
- **Nonperturbative** continuum method

Flow in theory space

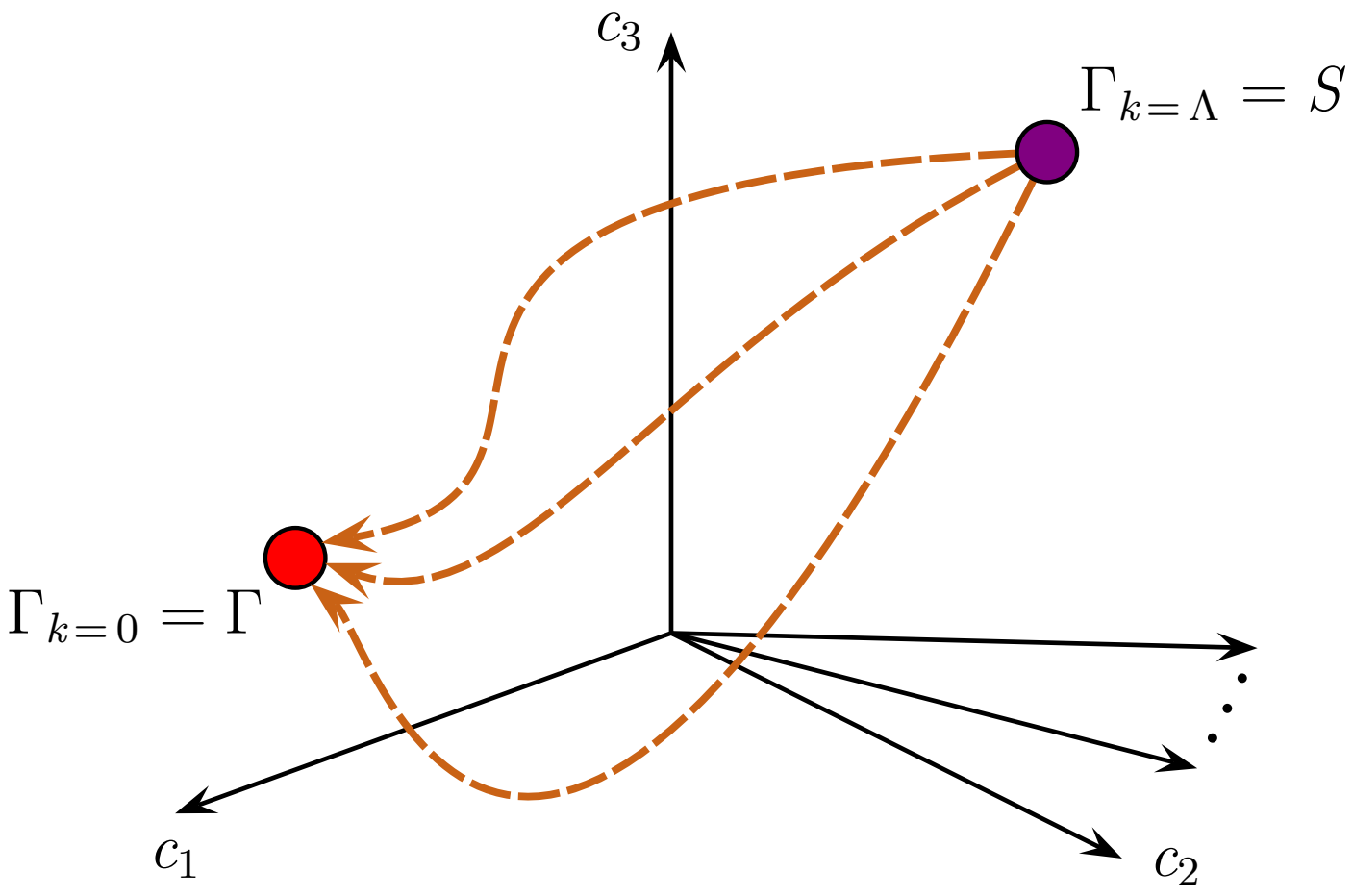

Figure 1: Theory space spanned by generic couplings.

$O(4)$ quark-meson model – truncations

- Local potential approximation (**LPA**), i.e., consider scale-dependent **effective potential**,

$$\Gamma_k = \int_x \left\{ \frac{1}{2} \left(\partial_\mu \sigma\right) \partial_\mu \sigma + \frac{1}{2} \left(\partial_\mu \vec{\pi}\right) \cdot \partial_\mu \vec{\pi} + U_k(\rho) - h_{\mathrm{ESB}} \sigma \right.$$
$$\left. + \bar{\psi} \left(\gamma_\mu \partial_\mu + y \Phi_5\right) \psi \right\}$$

- **LPA'**, i.e., include **wave-function renormalization**,

$$\Gamma_k = \int_x \left\{ \frac{Z_k^\sigma}{2} \left(\partial_\mu \sigma\right) \partial_\mu \sigma + \frac{Z_k^\pi}{2} \left(\partial_\mu \vec{\pi}\right) \cdot \partial_\mu \vec{\pi} + U_k(\rho) - h_{\mathrm{ESB}} \sigma \right.$$
$$\left. + \bar{\psi} \left(Z_k^\psi \gamma_\mu \partial_\mu + y \Phi_5 \right) \psi \right\}$$

Flow of the effective potential – LPA

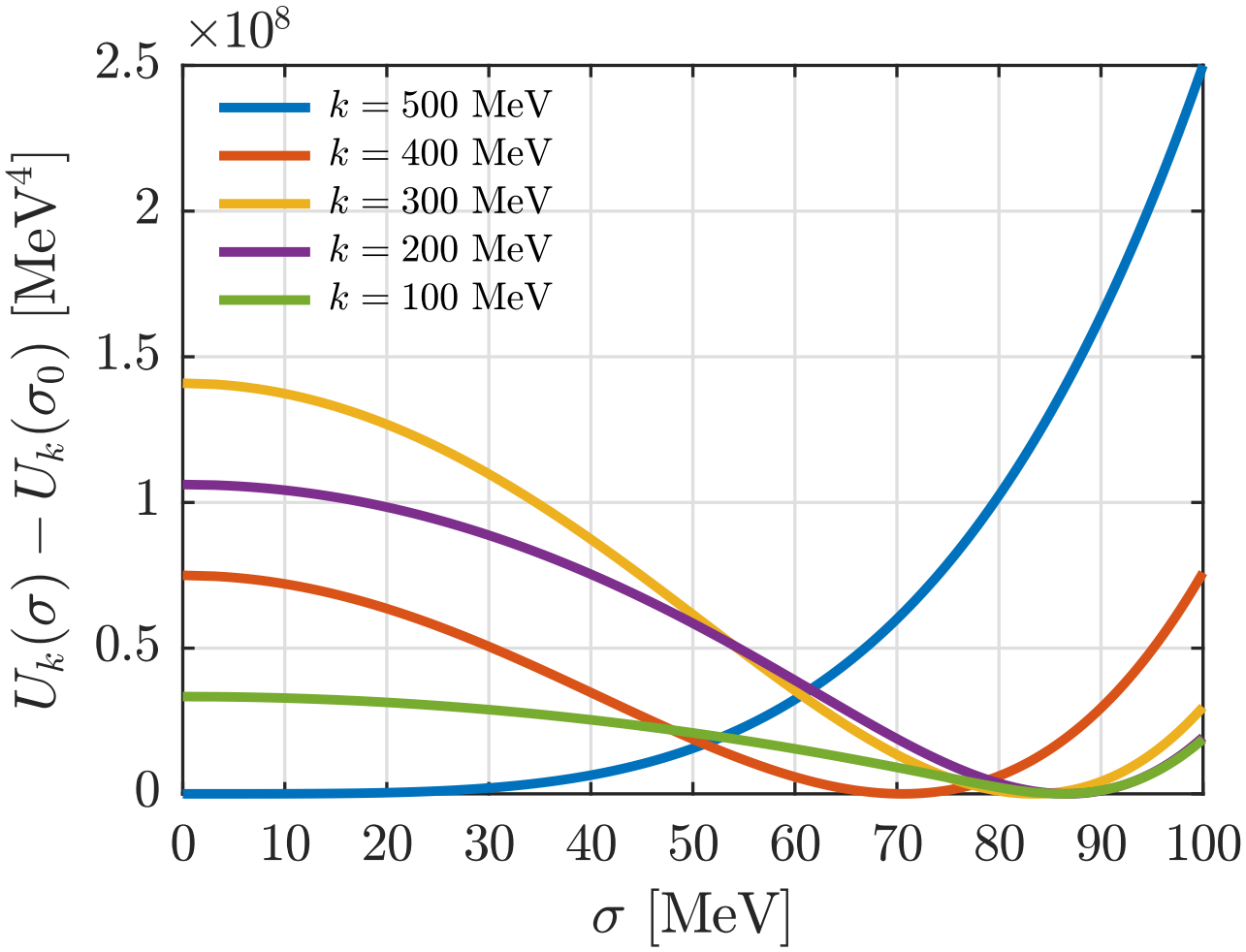

Figure 2: Scale evolution of the effective potential; grid discretization.

Remark: Technical details

- Analytic derivation of flow equations can be "expensive"
- Self-written routines and additional **software** used,

  DoFun [Huber, Braun '12]
  FormTracer [Cyrol, Mitter, Strodthoff '17]

- **Flow equations:** Set of coupled partial differential equations
- **Numerical solution:** Grid discretization, Taylor expansion, ...

$$U_k(\rho) = \sum_{n=1}^{N} \frac{\alpha_{n,k}}{n!} (\rho - \chi)^n$$

Remark: Grid vs. Taylor

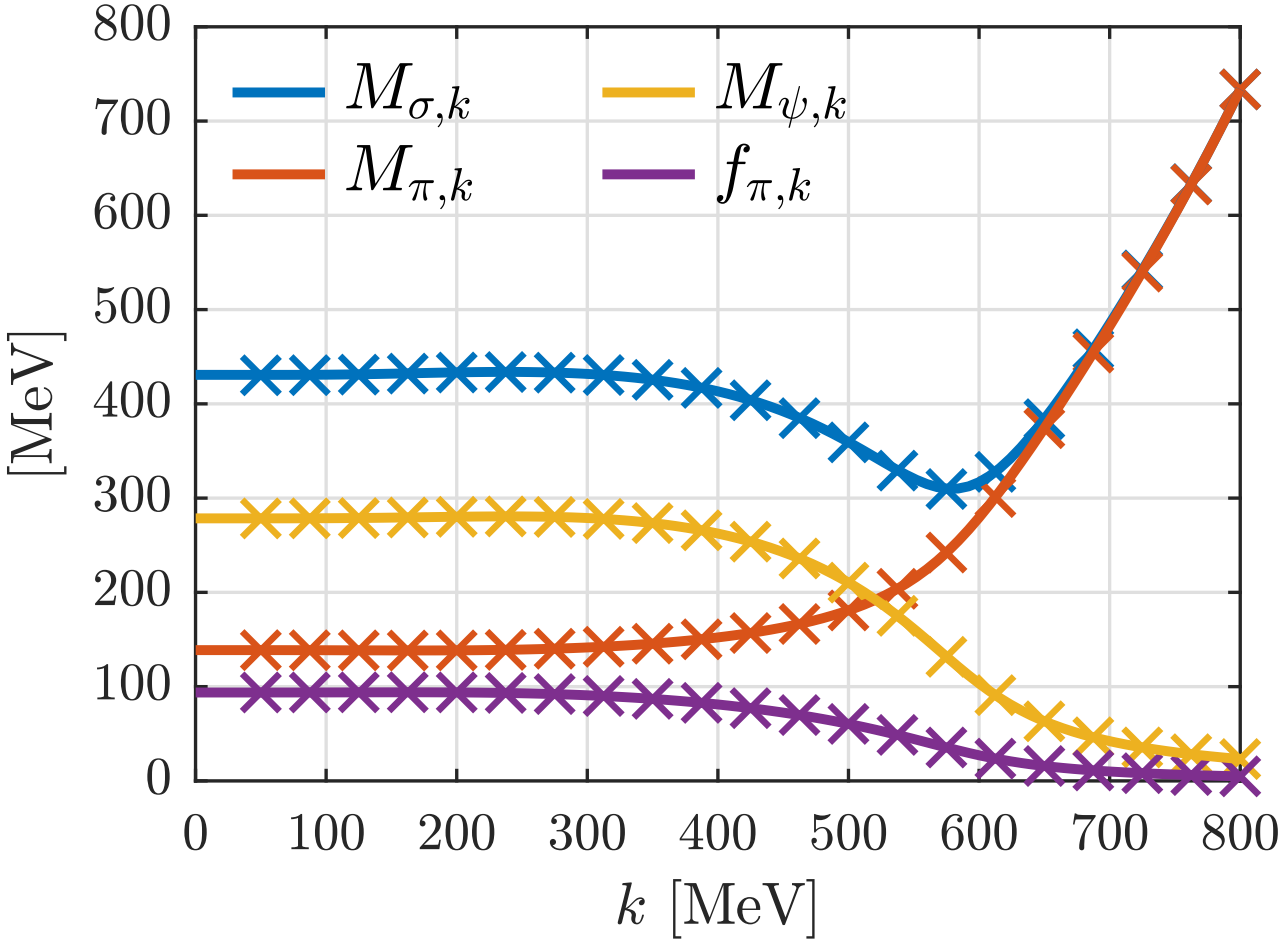

Figure 3: Scale evolution of meson and quark masses and the pion decay constant; lines: Taylor; crosses: grid.

Remark: Phase diagram – LPA

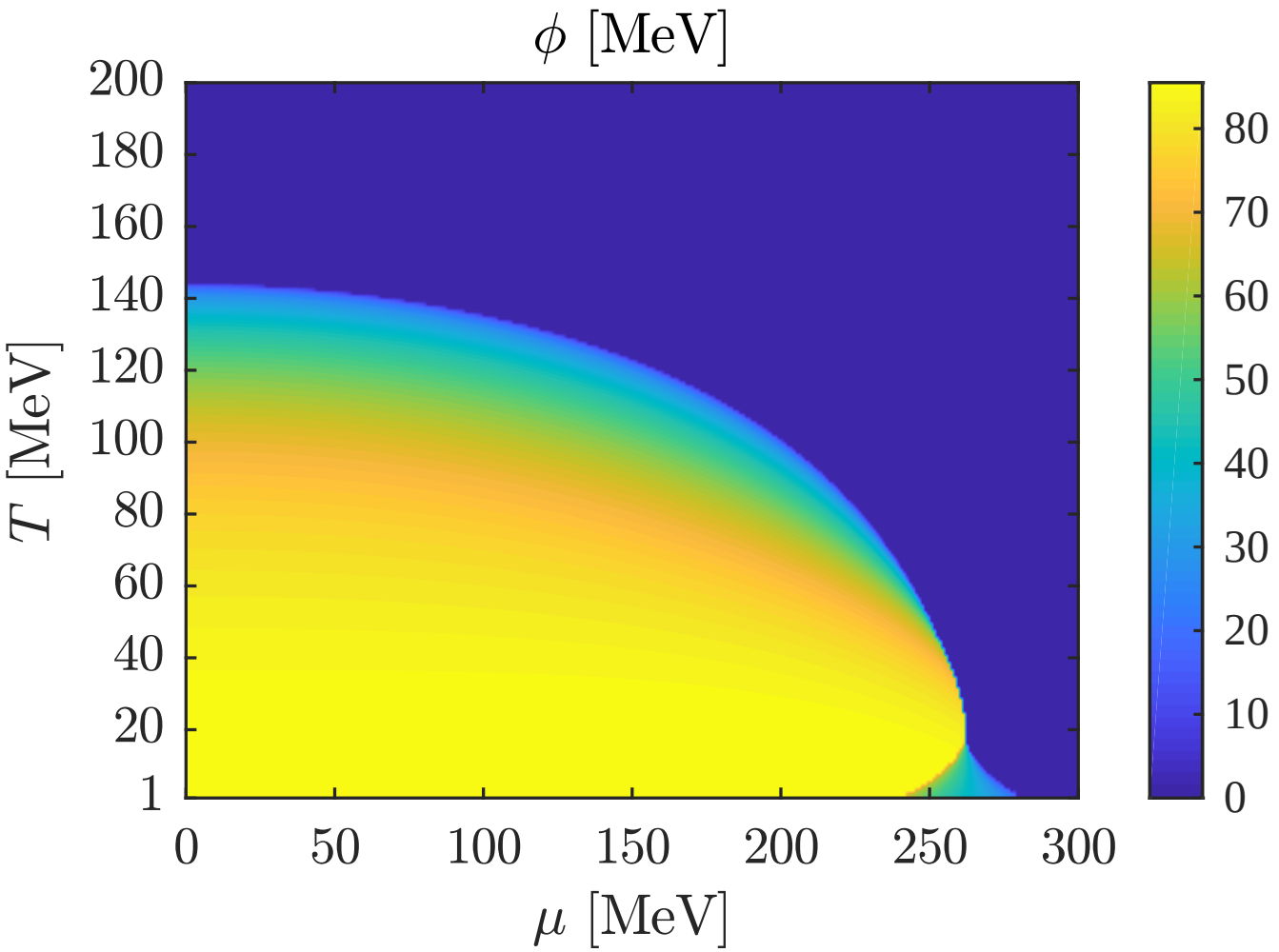

Figure 4: (μ, T) dependence of the v.e.v. ϕ in the chiral limit ($h_{\mathrm{ESB}} = 0$); grid method. Consistent with [Schaefer, Wambach '05].

Remark: Nonzero-temperature analysis

- Study of chiral-symmetry breaking in the eLSM with **vector and axial-vector mesons**,
  cf. [JE, Grahl, Rischke '15]
- Different symmetry aspects investigated
  (chiral limit, axial anomaly, ...)
- Phase-transition order **consistent** with other studies,
  cf. [Pisarski, Wilczek '84, etc.]

Effective action

- Introduce **low-energy couplings**,

$$
\begin{aligned}
\Gamma_k = \int_x \Bigg\{ & \frac{Z_k^\sigma}{2} \left(\partial_\mu \sigma\right) \partial_\mu \sigma + \frac{Z_k^\pi}{2} \left(\partial_\mu \vec{\pi}\right) \cdot \partial_\mu \vec{\pi} + U_k(\rho) - h_{\mathrm{ESB}} \sigma \\
& + C_{2,k} \left(\vec{\pi} \cdot \partial_\mu \vec{\pi}\right)^2 + Z_{2,k} \vec{\pi}^2 \left(\partial_\mu \vec{\pi}\right) \cdot \partial_\mu \vec{\pi} \\
& - C_{3,k} \left[\left(\partial_\mu \vec{\pi}\right) \cdot \partial_\mu \vec{\pi}\right]^2 - C_{4,k} \left[\left(\partial_\mu \vec{\pi}\right) \cdot \partial_\nu \vec{\pi}\right]^2 \\
& - C_{5,k} \vec{\pi} \cdot \left(\partial_\mu \partial_\mu \vec{\pi}\right) \left(\partial_\nu \vec{\pi}\right) \cdot \partial_\nu \vec{\pi} \\
& - C_{6,k} \vec{\pi}^2 \left(\partial_\mu \partial_\nu \vec{\pi}\right) \cdot \partial_\mu \partial_\nu \vec{\pi} \\
& - C_{7,k} \left(\vec{\pi} \cdot \partial_\mu \partial_\mu \vec{\pi}\right)^2 - C_{8,k} \vec{\pi}^2 \left(\partial_\mu \partial_\mu \vec{\pi}\right)^2 \\
& + \bar{\psi} \left(Z_k^\psi \gamma_\mu \partial_\mu + y \Phi_5 \right) \psi \Bigg\}
\end{aligned}
$$

- State-of-the-art truncation
- **Goal:** Compute the IR values of all k-dependent quantities

Renormalized quantities

- Renormalized fields:

$$\tilde{\sigma} = \sqrt{Z_k^\sigma}\sigma, \qquad \tilde{\vec{\pi}} = \sqrt{Z_k^\pi}\vec{\pi}, \qquad \tilde{\psi} = \sqrt{Z_k^\psi}\psi, \qquad \tilde{\bar{\psi}} = \sqrt{Z_k^\psi}\bar{\psi}$$

- (Squared) renormalized masses:

$$M_{\sigma,k}^2 = \frac{m_{\sigma,k}^2}{Z_k^\sigma}, \qquad M_{\pi,k}^2 = \frac{m_{\pi,k}^2}{Z_k^\pi}, \qquad M_{\psi,k}^2 = \frac{m_{\psi,k}^2}{\left(Z_k^\psi\right)^2}$$

- Renormalized **low-energy couplings**:

$$\tilde{C}_{i,k} = \frac{C_{i,k}}{\left(Z_k^\pi\right)^2} \quad i = 1, \ldots, 8, \qquad \tilde{Z}_{2,k} = \frac{Z_{2,k}}{\left(Z_k^\pi\right)^2}$$

Low-energy limit

- Use **equation of motion** in the IR,

$$\frac{\delta\Gamma}{\delta\tilde{\sigma}} = 0$$

- Yields effective **pion action**,

$$\begin{aligned}\Gamma_k = \int_x \Bigg\{ & \frac{1}{2}\left(\partial_\mu \tilde{\vec{\pi}}\right)\cdot\partial_\mu\tilde{\vec{\pi}} + \frac{1}{2}M^2_{\pi,k}\tilde{\vec{\pi}}^2 - \tilde{C}^{\text{total}}_{1,k}\left(\tilde{\vec{\pi}}^2\right)^2 \\ & + \tilde{C}^{\text{total}}_{2,k}\left(\tilde{\vec{\pi}}\cdot\partial_\mu\tilde{\vec{\pi}}\right)^2 + \tilde{Z}^{\text{total}}_{2,k}\,\tilde{\vec{\pi}}^2\left(\partial_\mu\tilde{\vec{\pi}}\right)\cdot\partial_\mu\tilde{\vec{\pi}} \\ & - \tilde{C}^{\text{total}}_{3,k}\left[\left(\partial_\mu\tilde{\vec{\pi}}\right)\cdot\partial_\mu\tilde{\vec{\pi}}\right]^2 - \tilde{C}^{\text{total}}_{4,k}\left[\left(\partial_\mu\tilde{\vec{\pi}}\right)\cdot\partial_\nu\tilde{\vec{\pi}}\right]^2 \\ & - \tilde{C}^{\text{total}}_{5,k}\,\tilde{\vec{\pi}}\cdot\left(\partial_\mu\partial_\mu\tilde{\vec{\pi}}\right)\left(\partial_\nu\tilde{\vec{\pi}}\right)\cdot\partial_\nu\tilde{\vec{\pi}} \\ & - \tilde{C}^{\text{total}}_{6,k}\,\tilde{\vec{\pi}}^2\left(\partial_\mu\partial_\nu\tilde{\vec{\pi}}\right)\cdot\partial_\mu\partial_\nu\tilde{\vec{\pi}} \\ & - \tilde{C}^{\text{total}}_{7,k}\left(\tilde{\vec{\pi}}\cdot\partial_\mu\partial_\mu\tilde{\vec{\pi}}\right)^2 - \tilde{C}^{\text{total}}_{8,k}\,\tilde{\vec{\pi}}^2\left(\partial_\mu\partial_\mu\tilde{\vec{\pi}}\right)^2 \Bigg\}\end{aligned}$$

Flow equations – examples

$$\partial_k U_k = \mathcal{V}^{-1}\Bigg(\frac{1}{2}$$

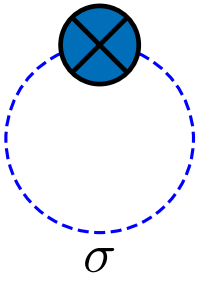

$$+\frac{1}{2}$$

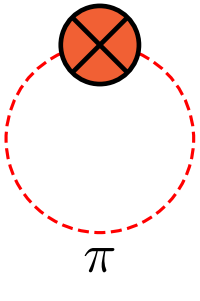

$$-$$

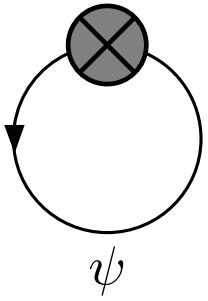

$$\Bigg),$$

$$\partial_k Z_k^\pi = \mathcal{V}^{-1}\left.\frac{\mathrm{d}}{\mathrm{d}p^2}\right|_{p^2=0}\Bigg(\frac{1}{2}$$

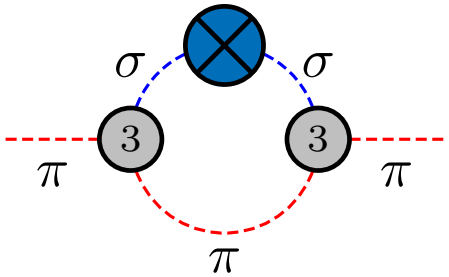

$$-\frac{1}{2}$$

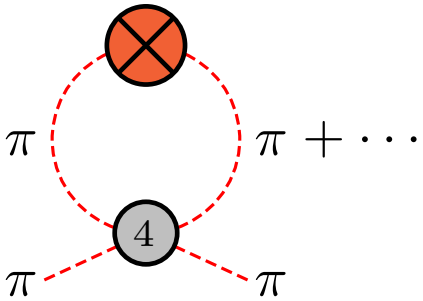

$$+\cdots\Bigg),$$

$$\partial_k C_{2,k} = \mathcal{V}^{-1}\left.\frac{\mathrm{d}}{\mathrm{d}p^2}\right|_{p^2=0}\Bigg(-\frac{1}{2}$$

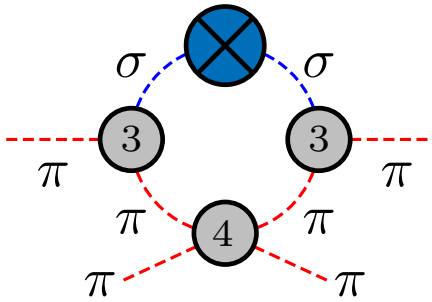

$$+\cdots\Bigg),$$

$$\vdots$$

Masses and pion decay constant

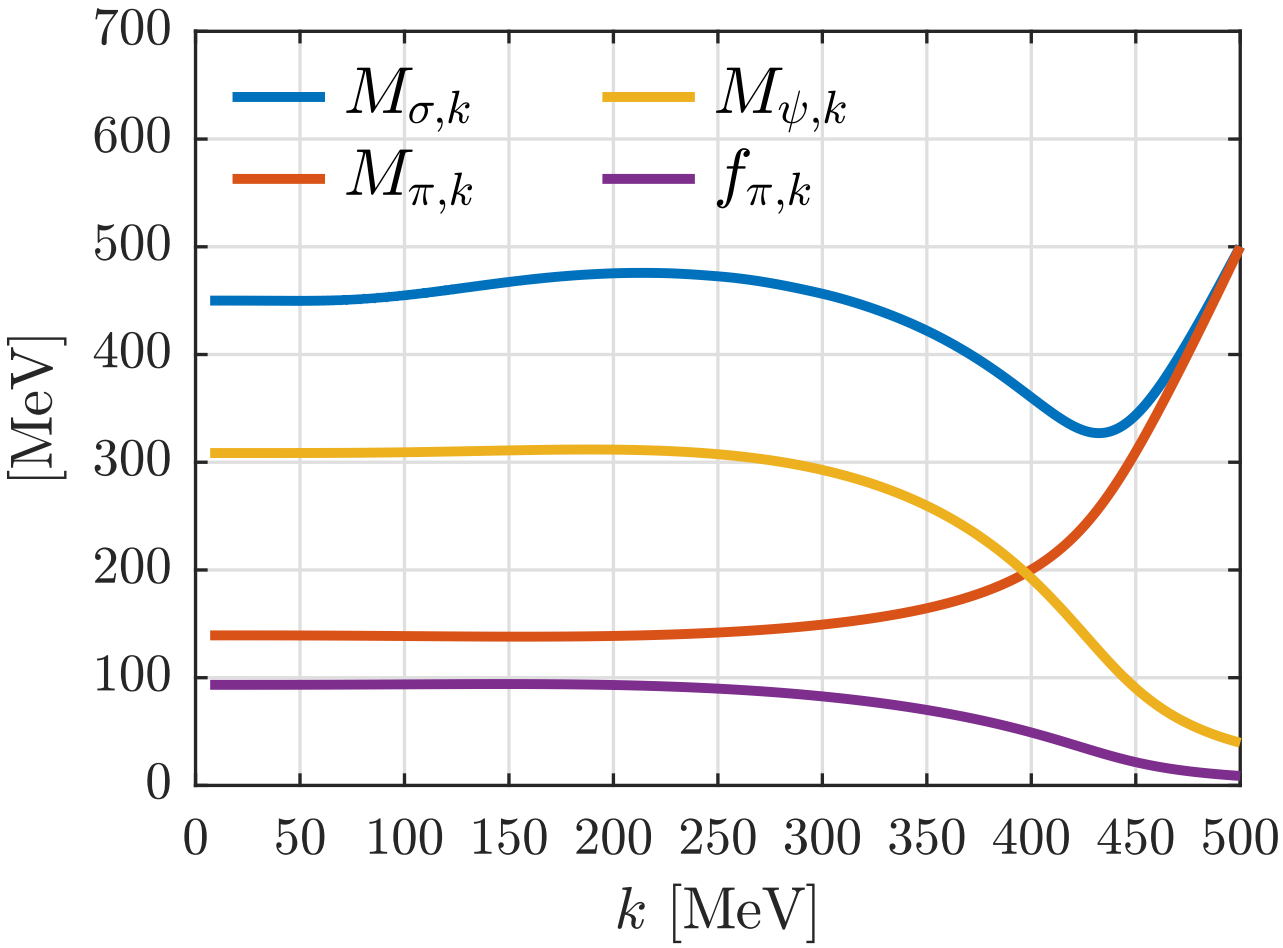

Figure 5: Scale evolution of the renormalized meson and quark masses and the pion decay constant; grid method;
[JE, Divotgey, Mitter, Rischke, PRD 98 (2018) no.1, 014024].

Wave-function renormalization

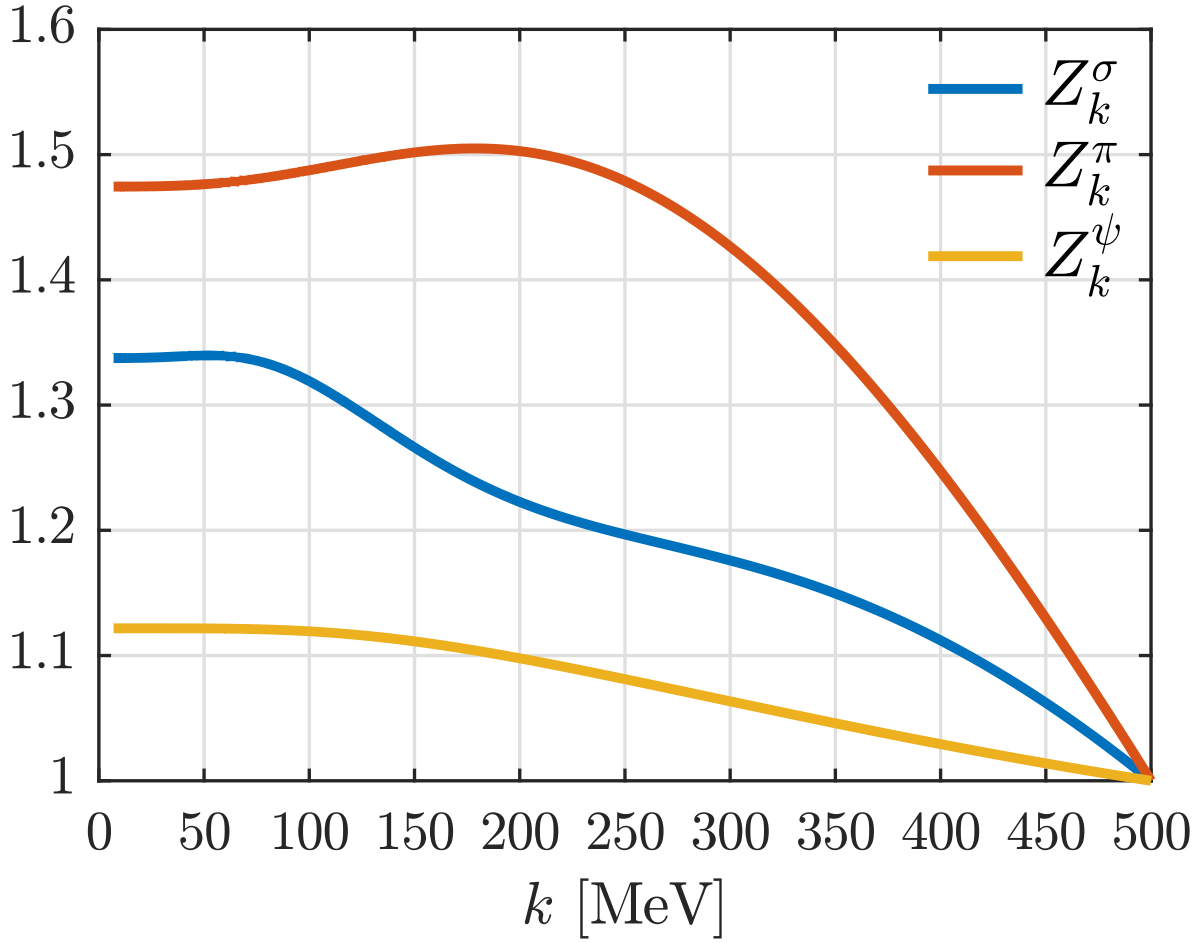

Figure 6: Scale evolution of the wave-function renormalization factors; grid method; [JE, Divotgey, Mitter, Rischke, PRD 98 (2018) no.1, 014024].

Low-energy couplings

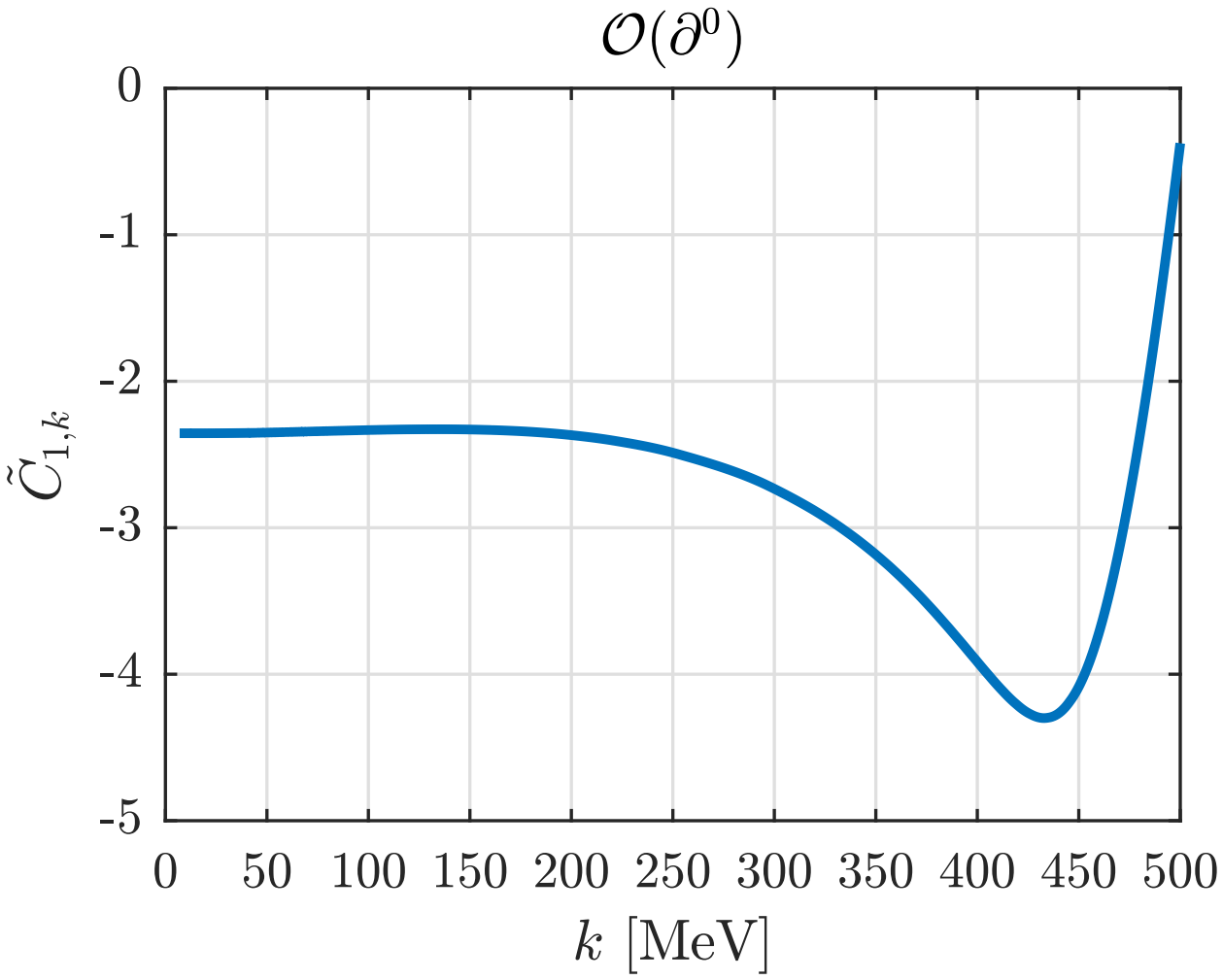

Figure 7: Scale evolution of the renormalized low-energy couplings (I); grid method; [JE, Divotgey, Mitter, Rischke, PRD 98 (2018) no.1, 014024].

Low-energy couplings

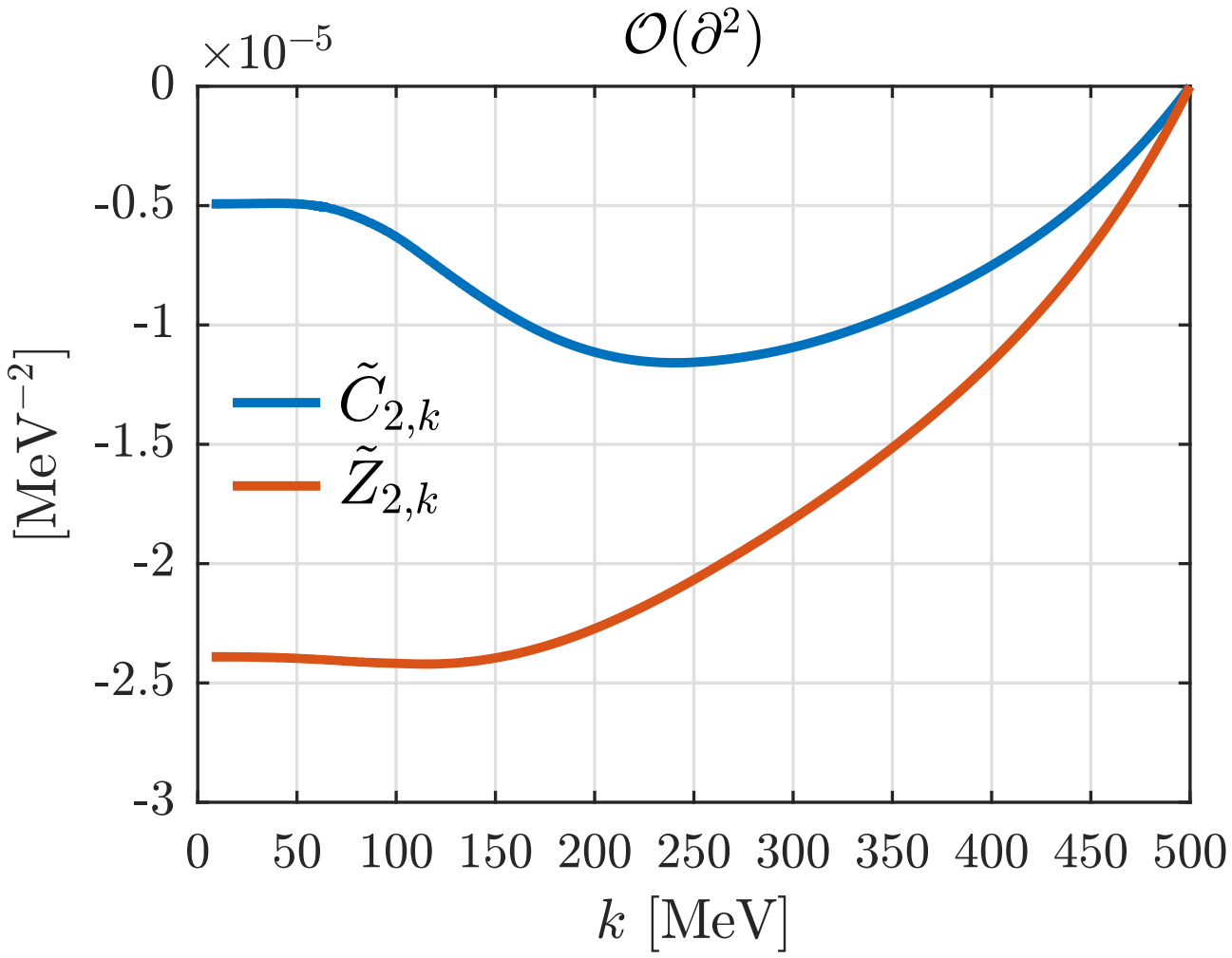

Figure 8: Scale evolution of the renormalized low-energy couplings (II); grid method; [JE, Divotgey, Mitter, Rischke, PRD 98 (2018) no.1, 014024].

Low-energy couplings

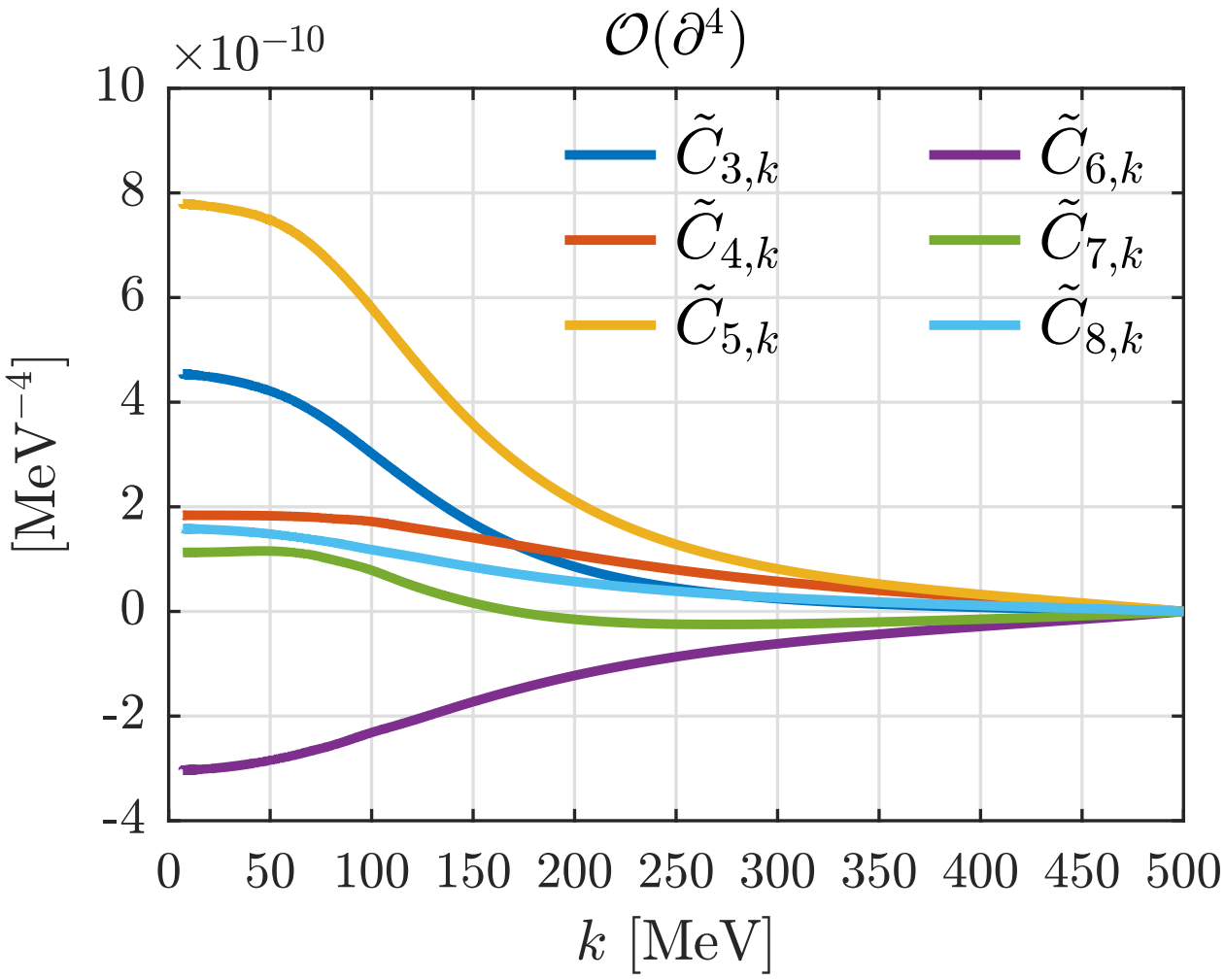

Figure 9: Scale evolution of the renormalized low-energy couplings (III); grid method; [JE, Divotgey, Mitter, Rischke, PRD 98 (2018) no.1, 014024].

Numerical results

Table 2: Low-energy couplings ($f_\pi = 93\ \mathrm{MeV}$);
[JE, Divotgey, Mitter, Rischke, PRD 98 (2018) no.1, 014024].

		FRG		
Coupling	**Tree level**	**Tree**	**Trunc**	**Total**
C_1	-0.2514	2.1063	-2.3550	-0.2487
$C_2\ [1/f_\pi^2]$	0.4054	0.3598	-0.0426	0.3172
$Z_2\ [1/f_\pi^2]$	–	–	-0.2068	-0.2068
$C_3\ [1/f_\pi^4] \times 10^2$	1.7311	1.5364	3.3946	4.9310
$C_4\ [1/f_\pi^4] \times 10^2$	–	–	1.3752	1.3752
$C_5\ [1/f_\pi^4] \times 10^2$	3.4621	3.0728	5.8294	8.9023
$C_6\ [1/f_\pi^4] \times 10^2$	–	–	-2.2697	-2.2697
$C_7\ [1/f_\pi^4] \times 10^2$	1.7311	1.5364	0.8439	2.3804
$C_8\ [1/f_\pi^4] \times 10^2$	–	–	1.1828	1.1828

Masses and pion decay constant – LPA'

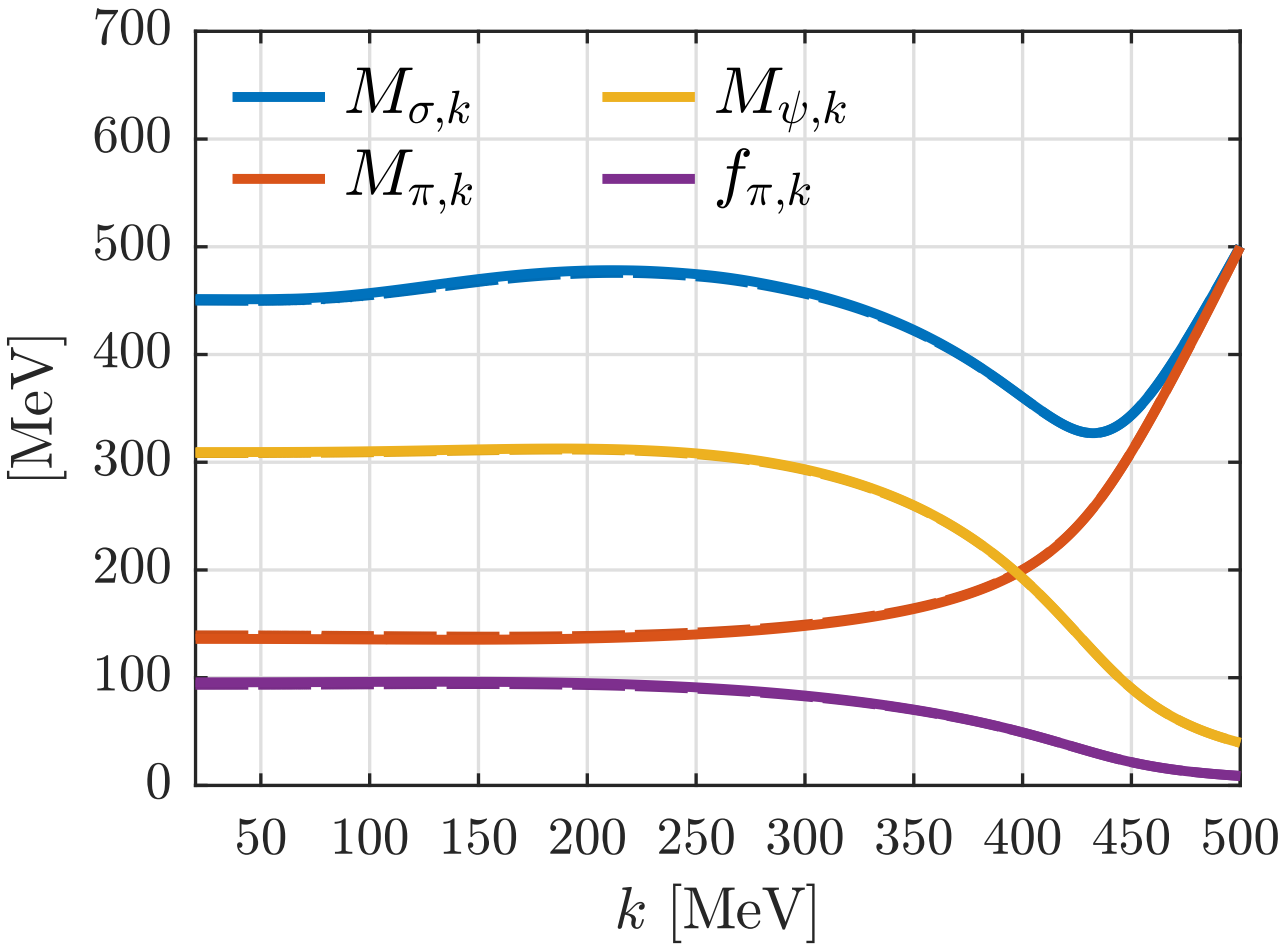

Figure 10: Renormalized masses and pion decay constant within the LPA' truncation. Dashed lines show the related results from Fig. 5; [JE, Divotgey, Mitter, Rischke, PRD 98 (2018) no.1, 014024].

Wave-function renormalization – LPA'

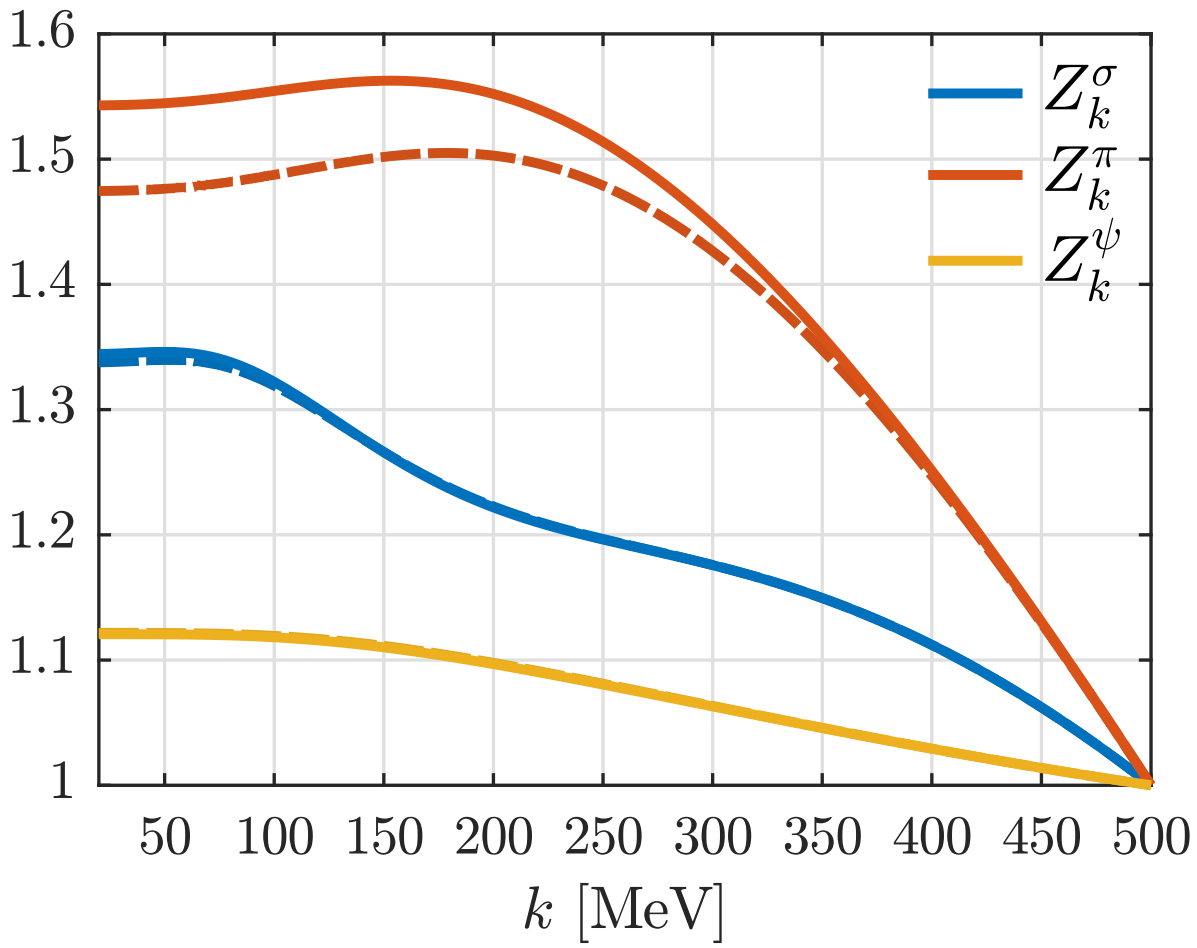

Figure 11: Wave-function renormalization factors within the LPA' truncation. Dashed lines show the related results from Fig. 6; [JE, Divotgey, Mitter, Rischke, PRD 98 (2018) no.1, 014024].

Work in progress

Effective action – full $O(4)$ symmetry

- $O(4)$ vector $\varphi = (\vec{\pi}, \sigma)$
- Include momentum-dependent mixed $\boldsymbol{\sigma\pi}$ **vertices** and $\boldsymbol{\sigma}$ **self-interactions**,

$$
\begin{aligned}
\Gamma_k = \int_x \Bigg\{ & \frac{Z_k}{2} \left(\partial_\mu \varphi\right) \cdot \partial_\mu \varphi + U_k(\rho) - h_{\mathrm{ESB}} \sigma \\
& + C_{2,k} \left(\varphi \cdot \partial_\mu \varphi\right)^2 + Z_{2,k} \, \varphi^2 \left(\partial_\mu \varphi\right) \cdot \partial_\mu \varphi \\
& - C_{3,k} \left[\left(\partial_\mu \varphi\right) \cdot \partial_\mu \varphi\right]^2 - C_{4,k} \left[\left(\partial_\mu \varphi\right) \cdot \partial_\nu \varphi\right]^2 \\
& - C_{5,k} \, \varphi \cdot \left(\partial_\mu \partial_\mu \varphi\right) \left(\partial_\nu \varphi\right) \cdot \partial_\nu \varphi \\
& - C_{6,k} \, \varphi^2 \left(\partial_\mu \partial_\nu \varphi\right) \cdot \partial_\mu \partial_\nu \varphi \\
& - C_{7,k} \left(\varphi \cdot \partial_\mu \partial_\mu \varphi\right)^2 - C_{8,k} \, \varphi^2 \left(\partial_\mu \partial_\mu \varphi\right)^2 \\
& + \bar{\psi} \left(Z_k^{\psi} \gamma_\mu \partial_\mu + y_k \Phi_5 \right) \psi \Bigg\}
\end{aligned}
$$

- Flow of Yukawa coupling taken into account

Masses and pion decay constant – full $O(4)$ symmetry

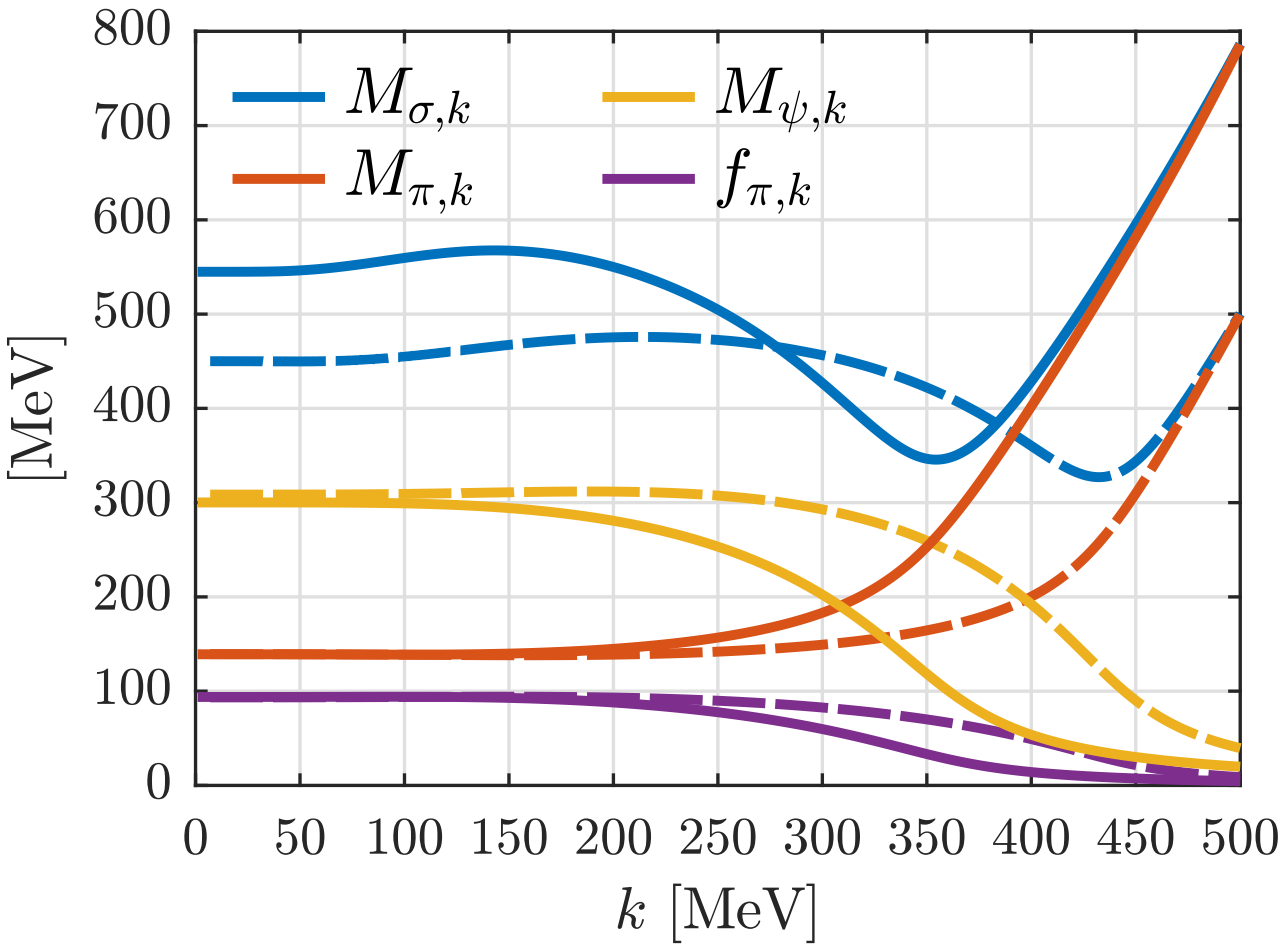

Figure 12: Renormalized masses and pion decay constant; Taylor-expansion method. Dashed lines show the related results from Fig. 5; [Eser, Divotgey, Mitter, in preparation].

Yukawa couplings – full $O(4)$ symmetry

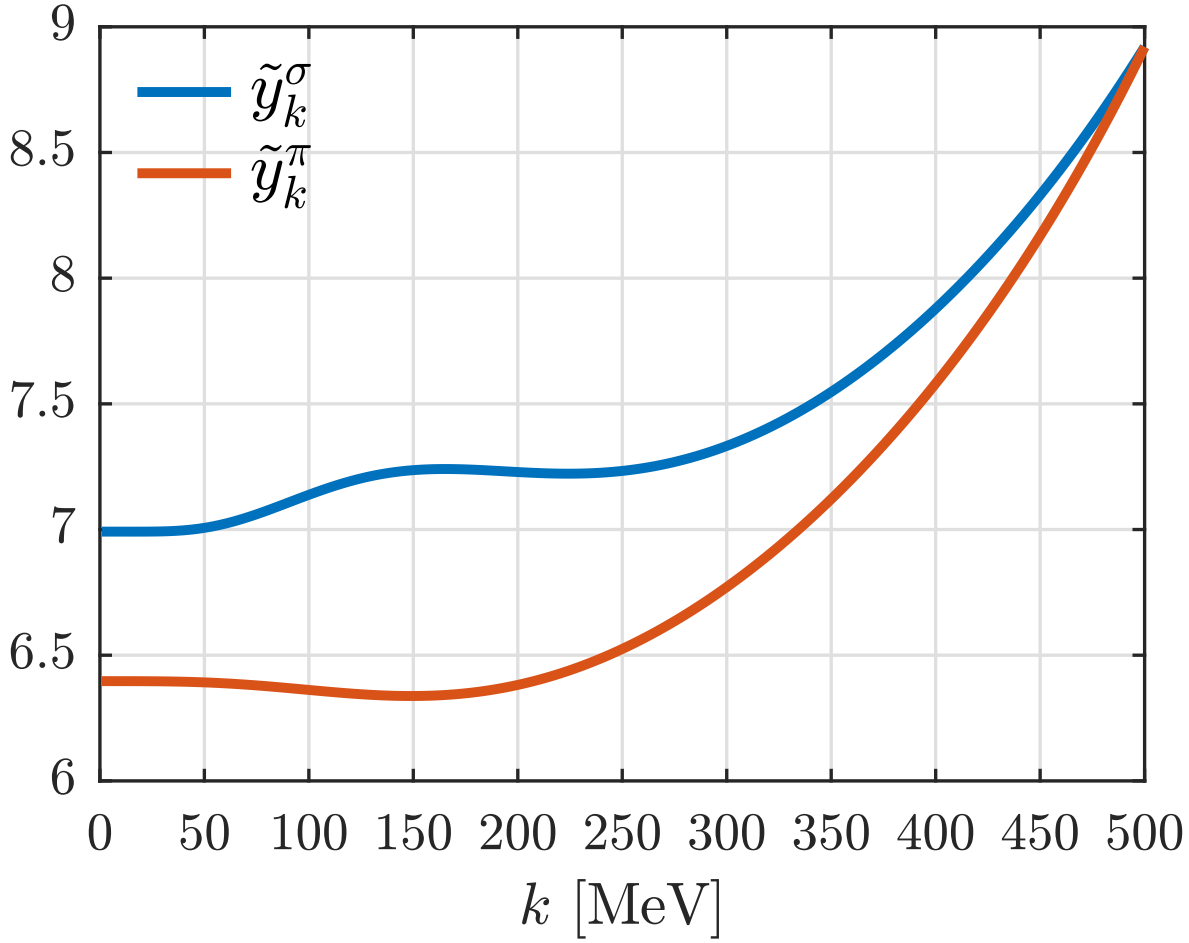

Figure 13: Scale evolution of the renormalized Yukawa couplings; Taylor-expansion method; [Eser, Divotgey, Mitter, in preparation].

Low-energy couplings – full $O(4)$ symmetry

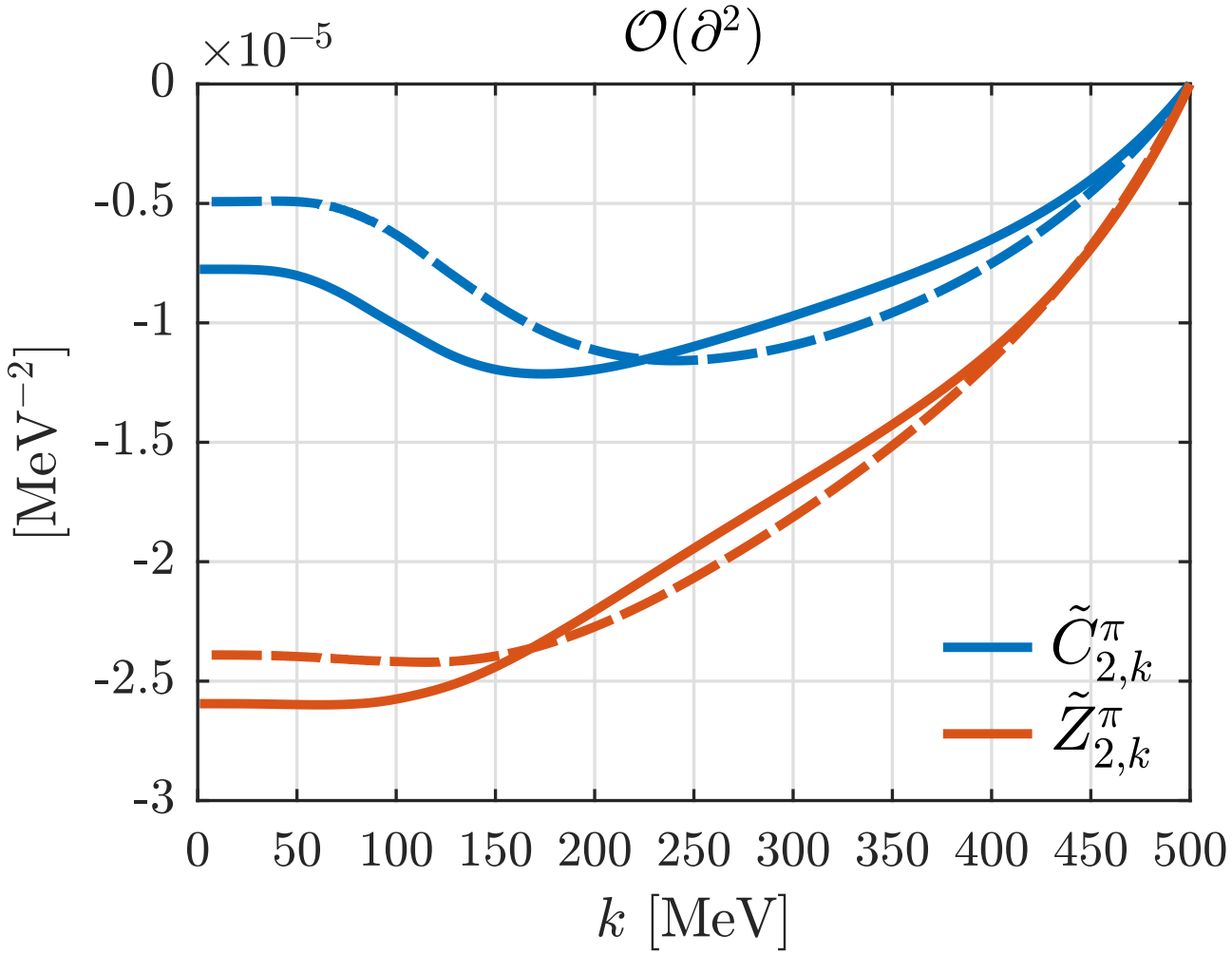

Figure 14: Renormalized low-energy couplings (I); Taylor-expansion method; Dashed lines show the related results from Fig. 8; [Eser, Divotgey, Mitter, in preparation].

Low-energy couplings – full $O(4)$ symmetry

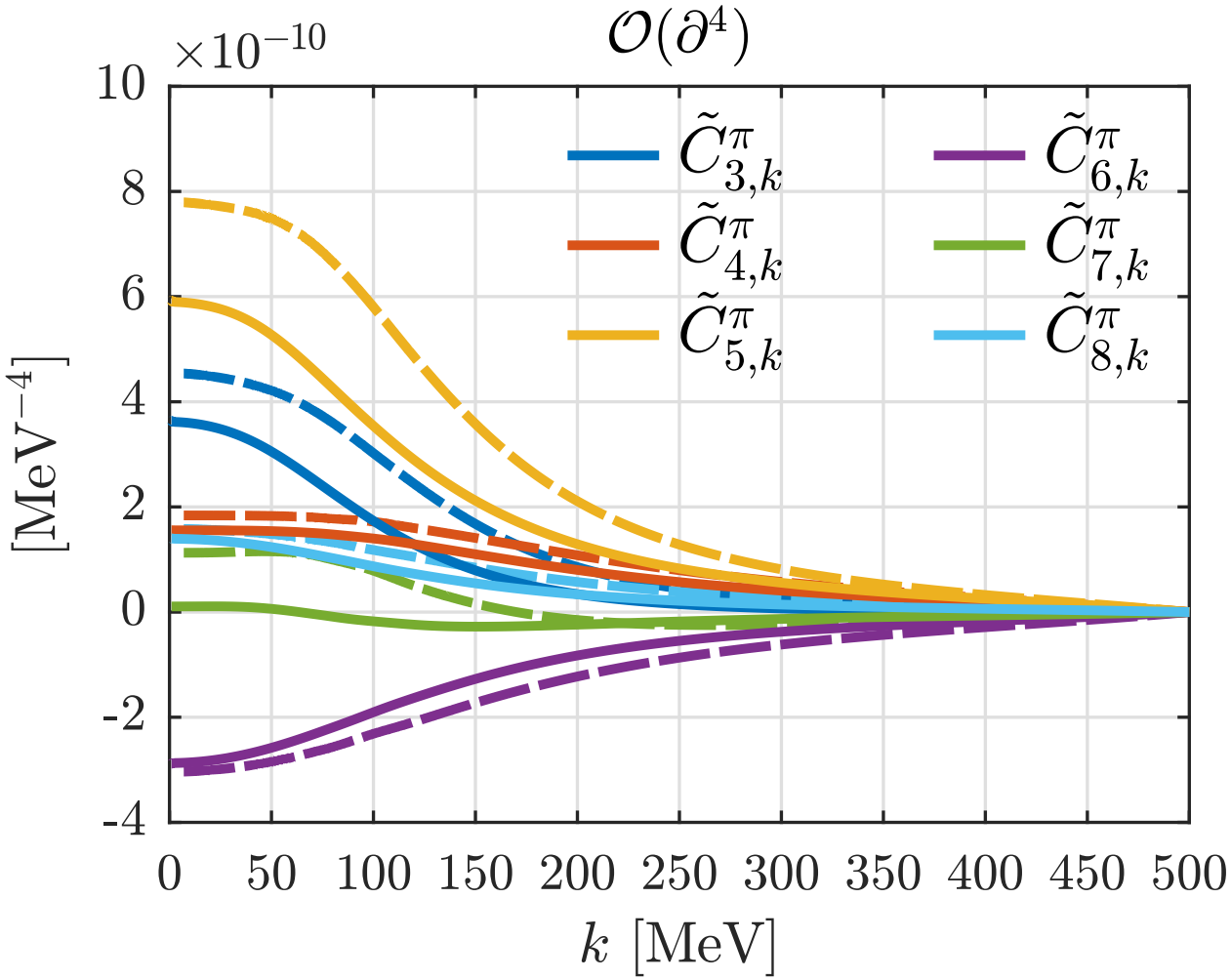

Figure 15: Renormalized low-energy couplings (II); Taylor-expansion method; Dashed lines show the related results from Fig. 9; [Eser, Divotgey, Mitter, in preparation].

Numerical results – full $O(4)$ symmetry

Table 3: Low-energy couplings ($f_\pi = 93\ \mathrm{MeV}$); full $O(4)$ symmetry.

		FRG		
Coupling	**Tree level**	**Tree**	**Trunc**	**Total**
C_1	-0.2568	2.9993	-3.2526	-0.2533
$C_2\ [1/f_\pi^2]$	0.4290	0.4732	-0.0671	0.4061
$Z_2\ [1/f_\pi^2]$	–	0.2069	-0.2244	-0.0175
$C_3\ [1/f_\pi^4] \times 10^2$	1.2495	-4.6110	2.7193	-1.8917
$C_4\ [1/f_\pi^4] \times 10^2$	–	–	1.1660	1.1660
$C_5\ [1/f_\pi^4] \times 10^2$	2.4990	-4.5794	4.4299	-0.1494
$C_6\ [1/f_\pi^4] \times 10^2$	–	1.9885	-2.1565	-0.1679
$C_7\ [1/f_\pi^4] \times 10^2$	1.2495	0.3885	0.0798	0.4684
$C_8\ [1/f_\pi^4] \times 10^2$	–	-0.9669	1.0485	0.0816

Symmetry constraints?

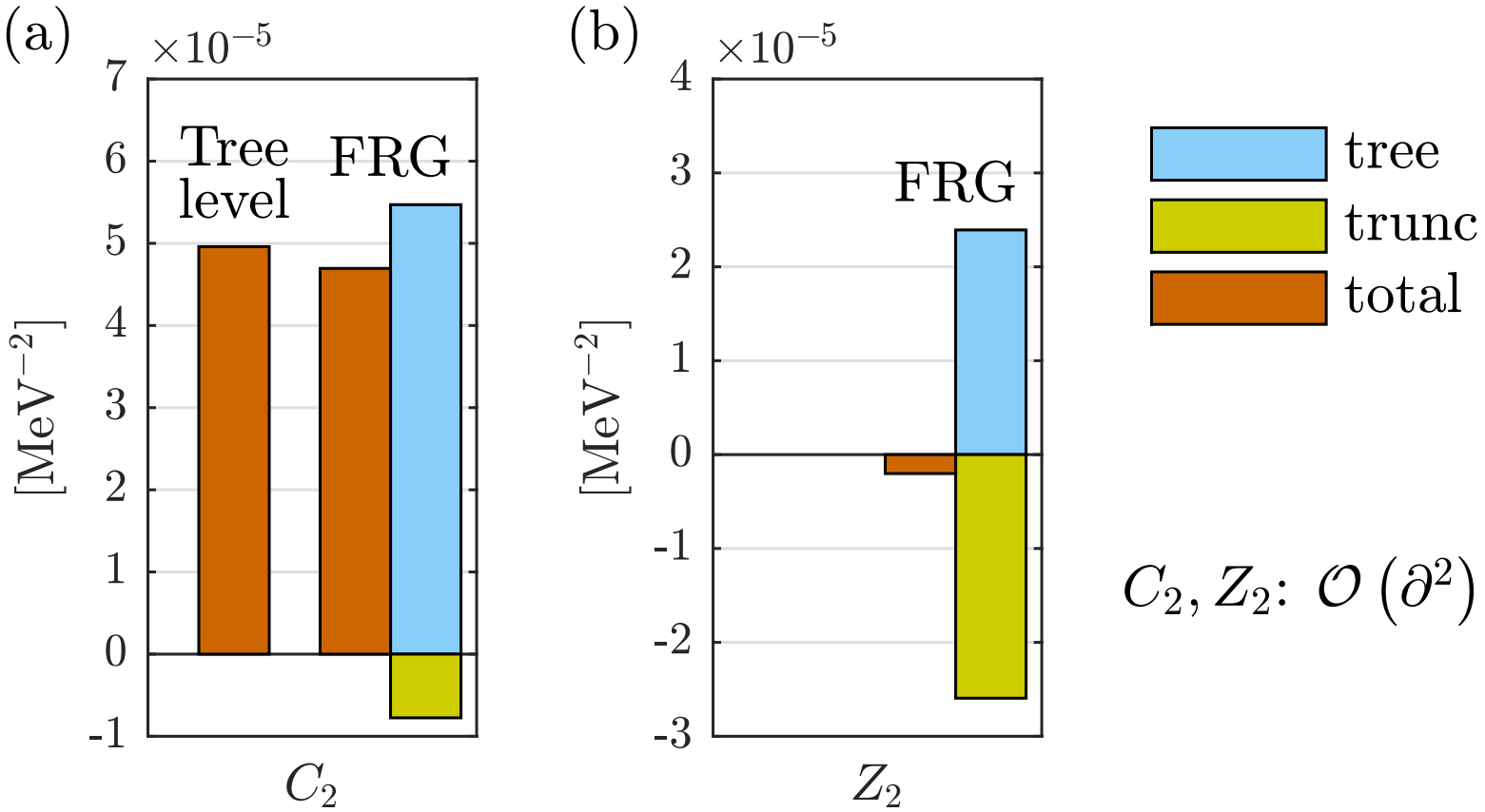

Figure 16: Bar representation of the low-energy couplings obtained from the tree-level and the FRG approaches.

Outlook

Functional QCD (fQCD)

- fQCD fluctuations:

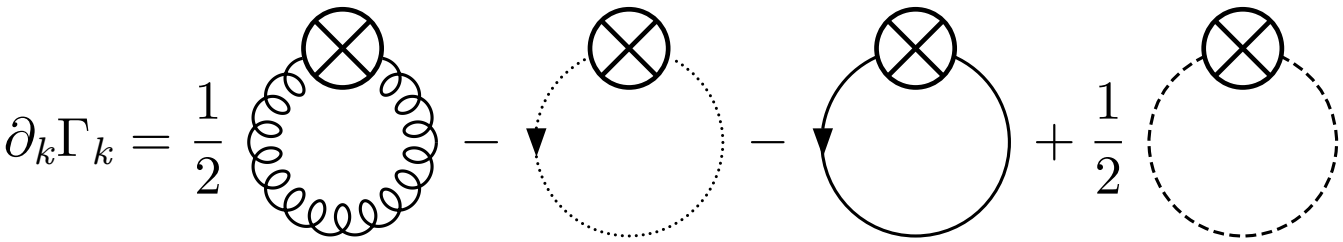

- Dynamical-hadronization technique
  [Gies, Wetterich '02; Mitter, Pawlowski, Strodthoff '15; Braun et al. '16]
- **Goal:** Determine low-energy couplings from fQCD
- **First approach:** Evaluate $O(4)$ equations on fQCD solution

fQCD solution

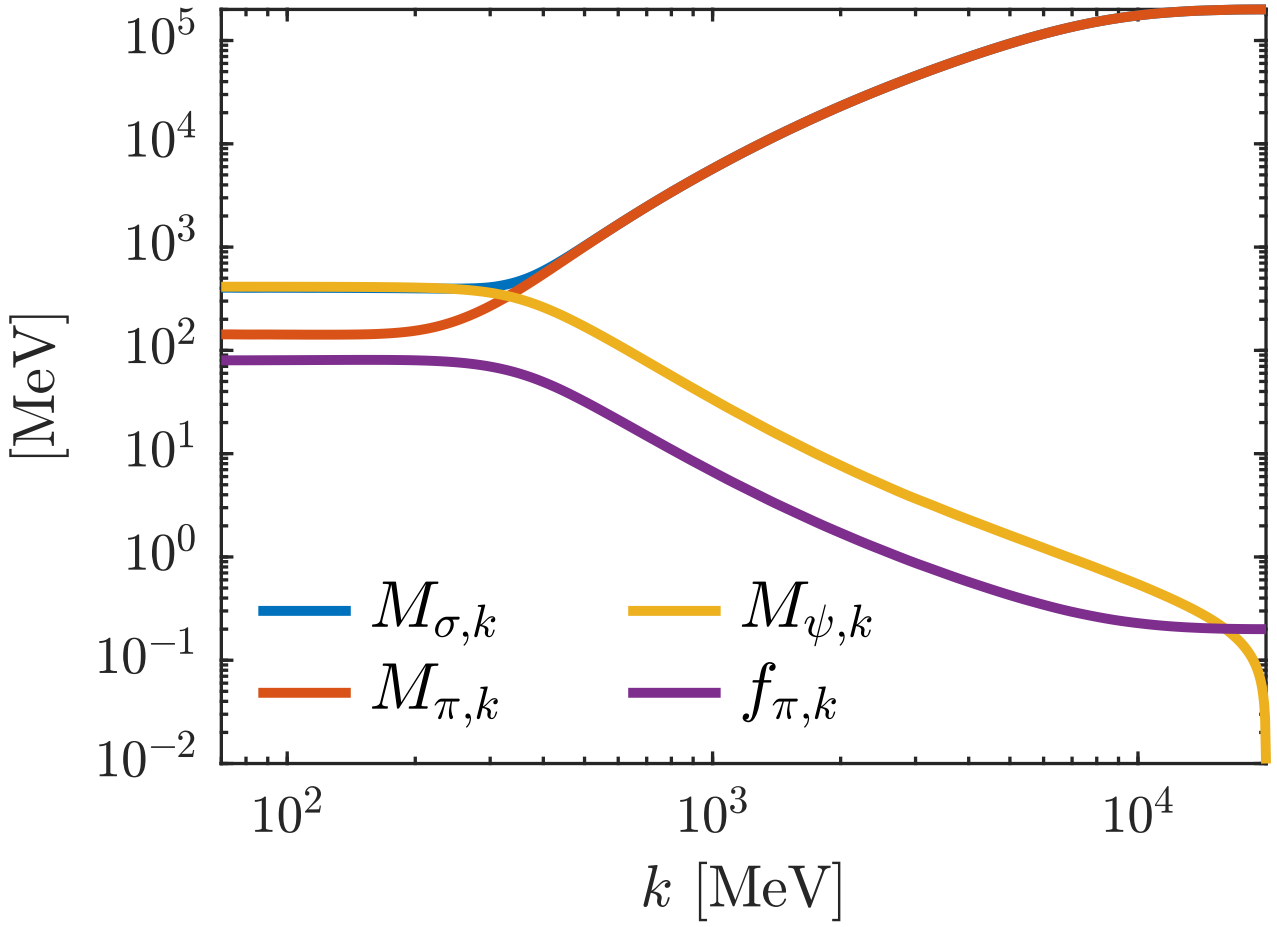

Figure 17: Renormalized meson and quark masses and the pion decay constant from fQCD (I).

fQCD solution

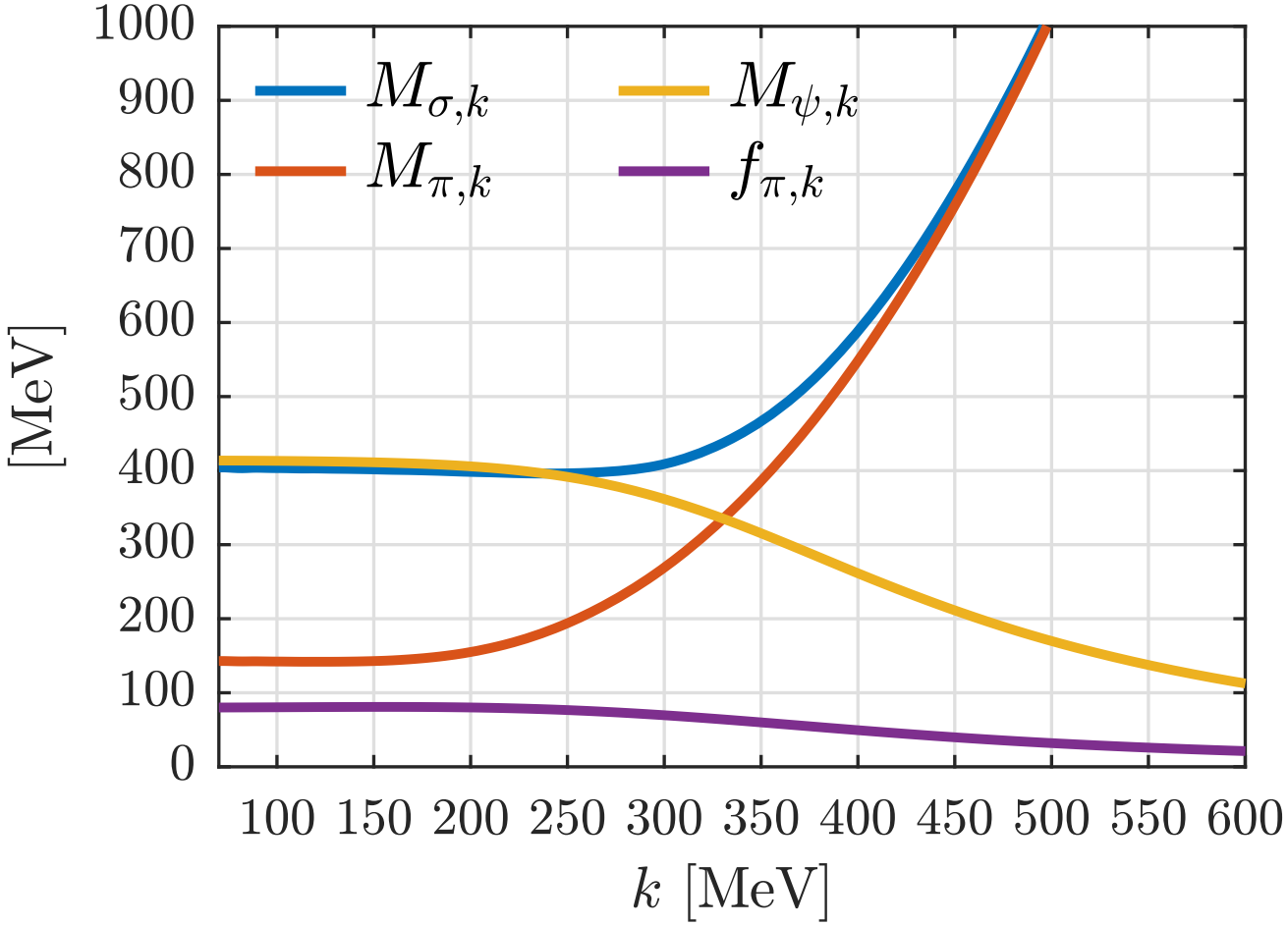

Figure 18: Renormalized meson and quark masses and the pion decay constant from fQCD (II).

fQCD solution

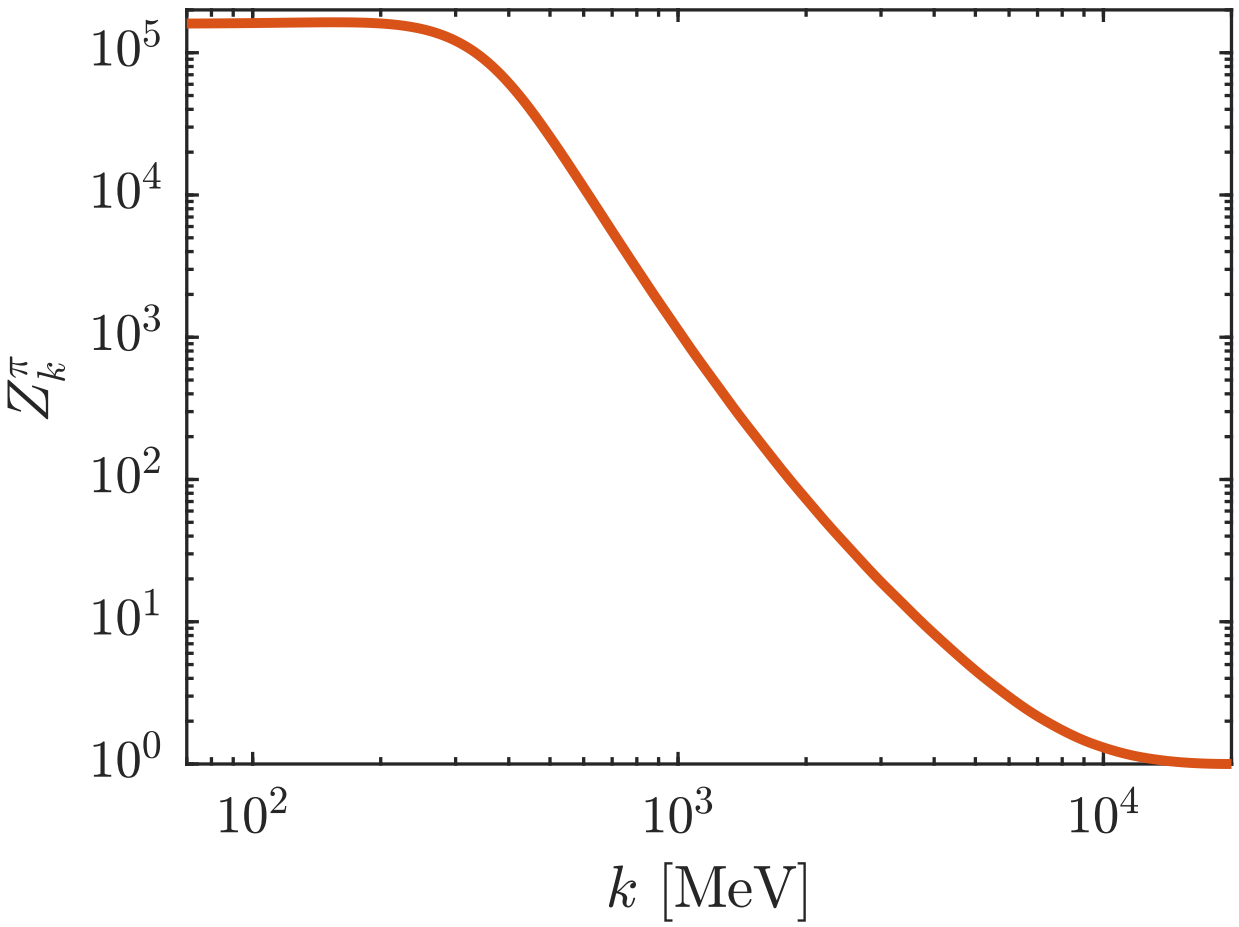

Figure 19: Pion wave-function renormalization from fQCD.

fQCD solution

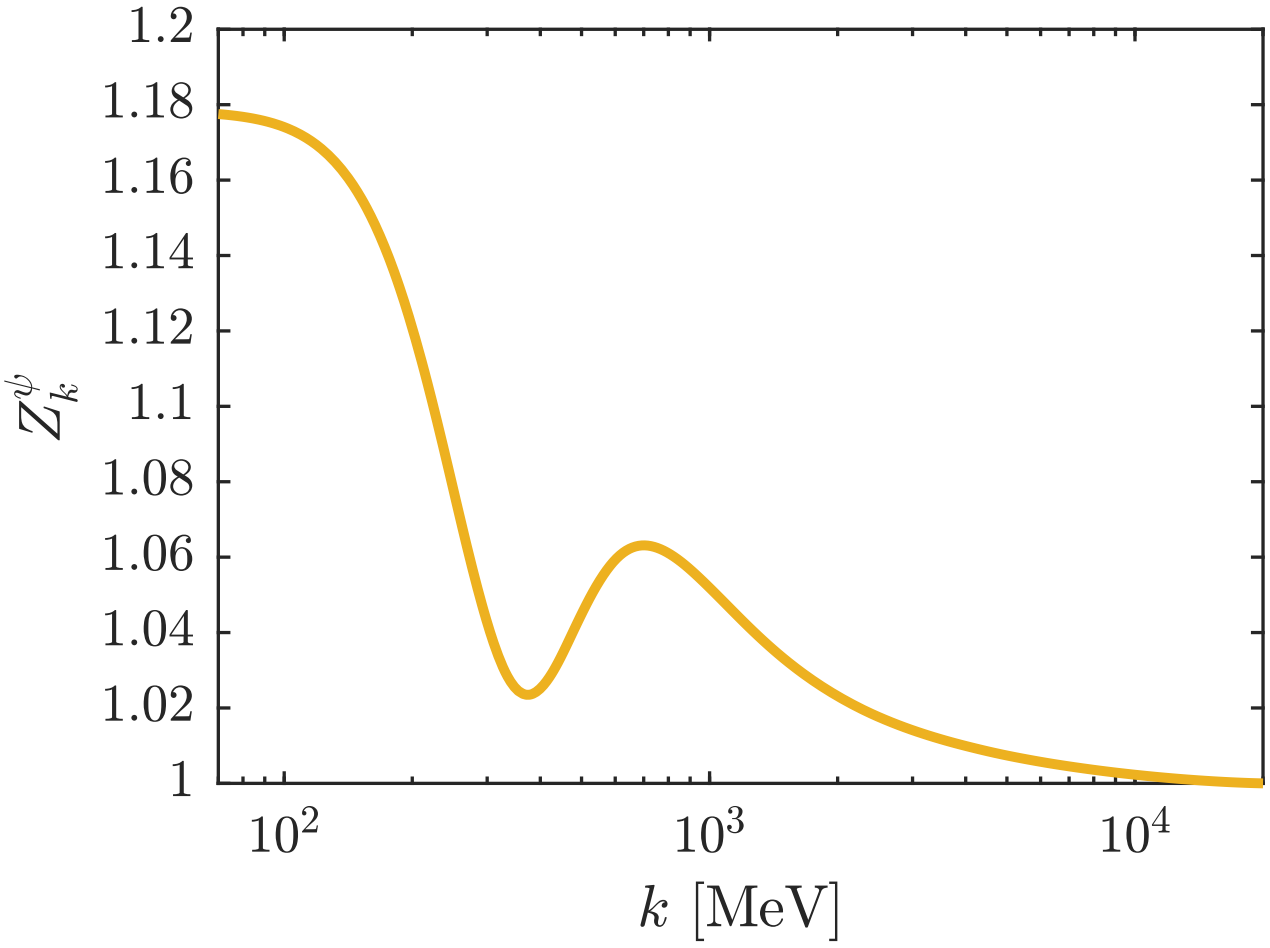

Figure 20: Quark wave-function renormalization from fQCD.

Low-energy couplings from fQCD

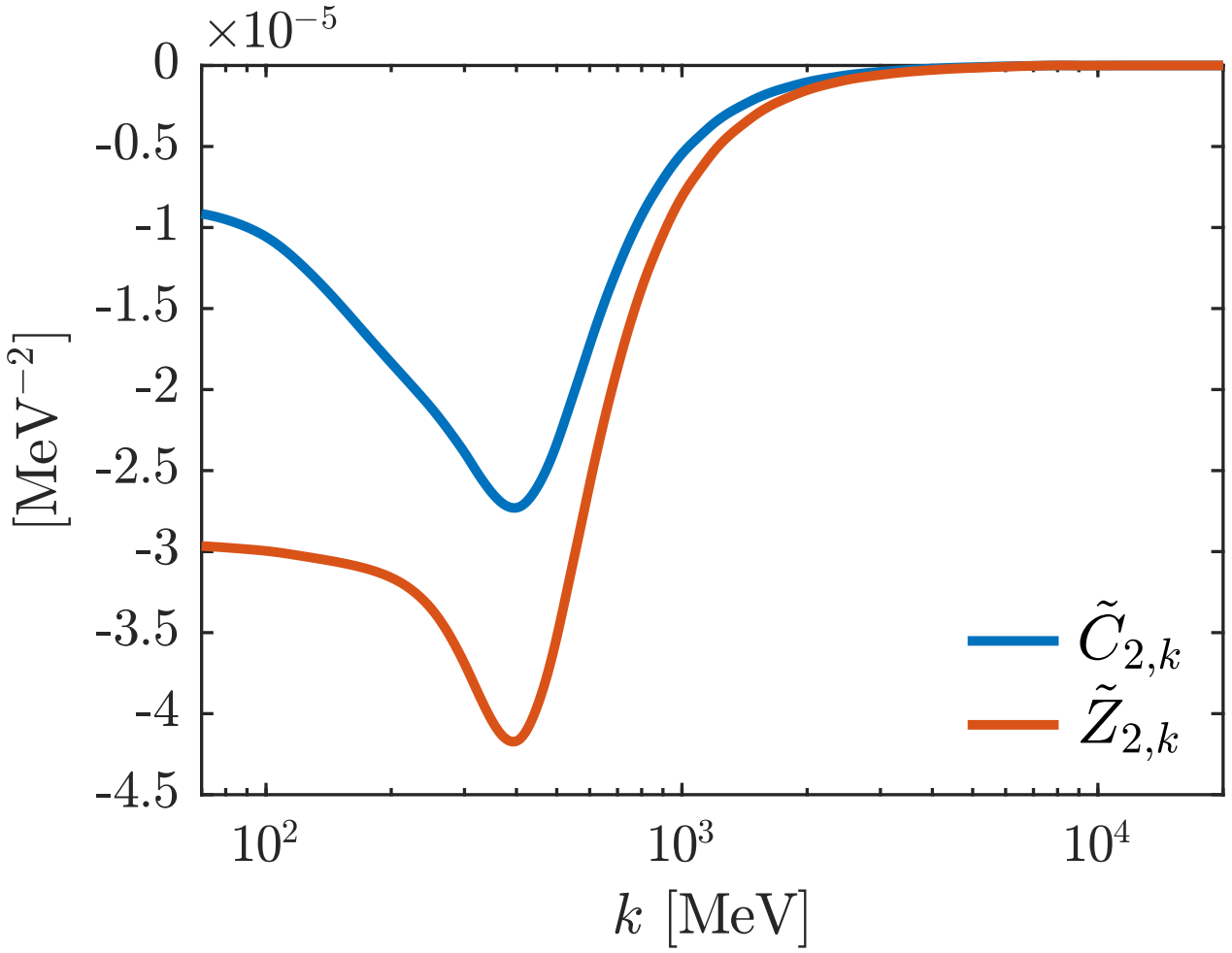

Figure 21: Low-energy couplings obtained from fQCD input (I).

Low-energy couplings from fQCD

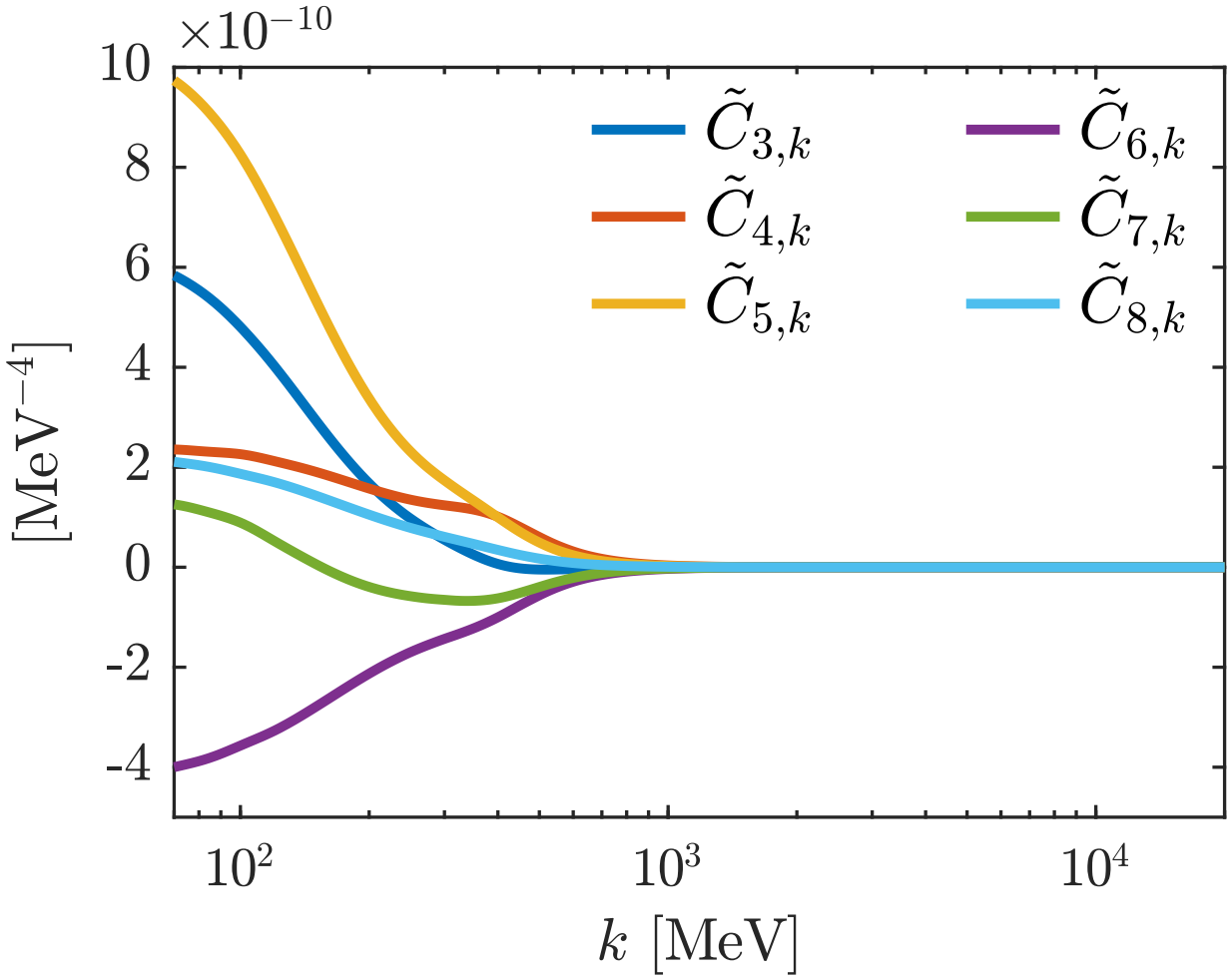

Figure 22: Low-energy couplings obtained from fQCD input (II).

Numerical results from fQCD

Table 4: Low-energy couplings from fQCD input.

		FRG	
Coupling	**Tree level**	$\boldsymbol{O(4)}$	**fQCD**
C_1	-0.2514	-0.2487	-0.3479
$C_2\ [1/f_\pi^2]$	0.4054	0.3172	0.4372
$Z_2\ [1/f_\pi^2]$	–	-0.2068	-0.2565
$C_3\ [1/f_\pi^4] \times 10^2$	1.7311	4.9310	7.1016
$C_4\ [1/f_\pi^4] \times 10^2$	–	1.3752	1.7625
$C_5\ [1/f_\pi^4] \times 10^2$	3.4621	8.9023	12.7534
$C_6\ [1/f_\pi^4] \times 10^2$	–	-2.2697	-2.9918
$C_7\ [1/f_\pi^4] \times 10^2$	1.7311	2.3804	3.6749
$C_8\ [1/f_\pi^4] \times 10^2$	–	1.1828	1.5770

Conclusions

Conclusions

Summary:

- Low-energy couplings of the eLSM at tree level in reasonable agreement with ChPT,
  cf. [Divotgey, Kovacs, Giacosa, Rischke '18]
- Low-energy limit of the $O(4)$ quark-meson model within the **FRG** confronted with a **tree-level estimate**,
  cf. [JE, Divotgey, Mitter, Rischke, PRD 98 (2018) no.1, 014024]
- **Discrepancy** between these approaches observed

Upcoming:

- Finalize analysis of the full $O(4)$-symmetric scenario
- Include vector mesons
- Compute low-energy limit from fQCD
- Confront the FRG calculation with ChPT